

Deep Imbalanced Time-series Forecasting via Local Discrepancy Density

Junwoo Park, Jungsoo Lee, Youngin Cho, Woncheol Shin, Dongmin Kim,
Jaegul Choo, and Edward Choi

Korea Advanced Institute of Science and Technology (KAIST), Daejeon, South Korea
{junwoo.park, bebeto, choyi0521, swc1905, tommy.dm.kim, jchoo,
edwardchoi}@kaist.ac.kr

Abstract. Time-series forecasting models often encounter abrupt changes in a given period of time which generally occur due to unexpected or unknown events. Despite their scarce occurrences in the training set, abrupt changes incur loss that significantly contributes to the total loss. Therefore, they act as noisy training samples and prevent the model from learning generalizable patterns, namely the normal states. Based on our findings, we propose a reweighting framework that down-weights the losses incurred by abrupt changes and up-weights those by normal states. For the reweighting framework, we first define a measurement termed *Local Discrepancy (LD)* which measures the degree of abruptness of a change in a given period of time. Since a training set is mostly composed of normal states, we then consider how frequently the temporal changes appear in the training set based on LD. Our reweighting framework is applicable to existing time-series forecasting models regardless of the architectures. Through extensive experiments on 12 time-series forecasting models over eight datasets with various in-output sequence lengths, we demonstrate that applying our reweighting framework reduces MSE by 10.1% on average and by up to 18.6% in the state-of-the-art model.

Keywords: Time-series forecasting · Data imbalance · Noisy samples.

1 Introduction

As vast records are collected over time in diverse fields, the demand to predict the future based on the previous sequential data has led to efforts to solve the time-series forecasting problem in various applications such as energy [1], economics [7], traffic [23], weather [21], environment pollution [6] and mechanical system monitoring [29]. Previous studies focused on addressing the well-known challenges of time-series forecasting such as finding reliable dependencies from intricate and entangled temporal patterns [25,19] or extending the forecasting time (i.e., long-term forecasting) [30,17,25,29]. For example, recent studies focused on improving the Transformer-based [22] models to address the long-term forecasting by taking the advantage of the long-term capacity of the self-attention mechanism and reducing quadratic computational costs [15,29,25,17].

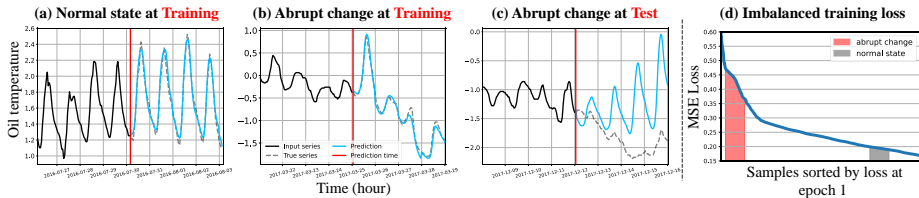


Fig. 1. We observe that the state-of-the-art forecaster correctly predicts the target values during the training phase over both (a) normal states and (b) abrupt changes, respectively. However, (c) illustrates that the model fails to correctly predict the abrupt change during the test phase. (d) shows imbalanced loss when the training samples are sorted by MSE loss of each sample in the early training phase. Our important finding is that the training samples with abrupt change (b) occupy the large portion of total loss. On the other hand, training samples within the normal states (a) have a relatively small loss. This leads the model to focus less on the normal states during training.

Despite the remarkable improvements of the previous studies, even the state-of-the-art models take little account of the *abrupt changes* in time-series data. Abrupt change refers to the drastic change of target values (either increase or decrease) beyond the extent of the changes observed in the recent past. These abrupt changes are challenging, if not impossible to predict based solely on previous observations of the target variable, as they are generally caused by unexpected and external events (*e.g.*, natural disaster and war). Such changes break the auto-correlation structures, the periodic relationships between target variables, which are essential for a time-series forecaster to predict futures. One straightforward remedy is to laboriously collect external variables (*e.g.*, annotations of external events) and enforce a model to learn the relationship between the collected variables and the target variables (*i.e.*, cross-correlation). However, utilizing additional variables without thorough verification causes the model to learn a spurious correlation between variables, which worsens the generalization ability. Moreover, some abrupt changes have unknown causes (*e.g.*, sensor malfunction), which cannot be addressed by simply collecting external variables.

While forecasting abrupt changes is known to be challenging [18,10], even worse, another significant issue of abrupt changes is that they limit the generalization performance of forecasting models during the test phase. Deep learning models are known to correctly predict all training samples regardless of the noisy labels by simply memorizing them (*i.e.*, overfitting) [27]. Our finding is that recent time-series forecasting models can easily memorize even abrupt changes in which the output sequence shows the different temporal characteristics (*e.g.*, mean, variance, and periodic structure) with the input sequence as shown in Figure 1. To be more specific, Figure 1(a) and (b) show that the model correctly predicts the target values during the training phase in both normal states (*i.e.*, trend or periodicity of input sequence maintained in the output sequence) and abrupt changes, respectively. However, Figure 1(c) illustrates that the model fails to correctly predict the abrupt change during the test phase. The main reason is that the model is heavily overfitted to the abrupt changes since they

take a significant portion of the total loss value compared to the ones in normal states (Figure 1(d)). Therefore, we propose a simple yet effective reweighting

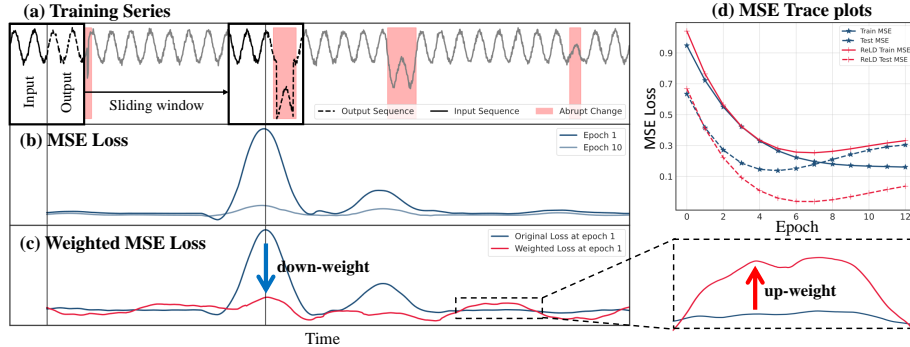


Fig. 2. (a) We trained a model with a training series including four abrupt changes (red-shaded regions). (b) While the losses caused by the abrupt changes are considerably high in the early training phase, they are reduced significantly after several epochs of training. (d) After the losses by abrupt changes are decreased, however, we observe that the test losses rather increase, implying the degraded generalization capability. (c) We mitigate such an issue by proposing a reweighting framework that down-weights the losses of samples containing the abrupt changes (blue arrow) and up-weights normal samples (red arrow). (d) The model trained with our proposed reweighting framework achieves lower test MSE compared to that of the model without our framework.

framework that encourages the model to balance the imbalanced loss between abrupt changes and normal states. Generally, time-series datasets do not provide explicit labels as to when the abrupt changes occur. Moreover, explicitly bisecting time stamps into abrupt changes and normal states is challenging since the definition of abrupt change may be vague depending on perspectives. Thus, we define a measure called *Local Discrepancy* (LD) which is used to determine how much a change in a given period of time is abrupt. By sliding a fixed-size window over the training time-series data, we compute the statistical difference between the in-output sequences as LD. Then, based on the observation that abrupt changes rarely appear in the training samples while normal states comprise the majority of the training set, we count the frequency of temporal changes based on LD. We divide the LD values into a predefined number of bins which are smoothed by kernel density estimation (*i.e.*, estimated LD density). By obtaining low LD density for the abrupt changes and high ones for the normal states, we *reweight* loss values proportional to the estimated **LD Density**, which we term our method as *ReLD*. This enables to emphasize the normal states which are the ones a model should learn for enhancing the forecasting capability. In summary, the main contributions of our work are as follows:

- We reveal that the abrupt changes significantly degrade the time-series forecasting performance by taking most of the loss values.

- We propose a simple yet effective reweighting framework that adjusts the balance of the loss based on LD density, namely ReLD.
- Our reweighting framework consistently improves the performance of twelve existing time-series models on eight datasets, which reduces MSE by 10.1% on average and up to 18.6% when applied to the state-of-the-art model.
- ReLD also outperforms methods addressing the noisy samples such as smoothing, outlier filtering, and error-based baselines with a significant margin.

2 Related Work

2.1 Deep Learning Models for Time-series Forecasting

Deep learning-based models that have shown successful results in various domains have been actively applied to the time-series forecasting problem, which was originally dominated by classic statistical-based models [2]. Recent studies focused on extending forecasting time [30,17,25,29]. As the demand for long-term planning and early warning in the real-world applications has increased, long-term forecasting has become essential. Thus, transformer-based forecasting models, which are known to effectively learn global temporal patterns, have emerged. These studies proposed sparse attention mechanisms to reduce the computational cost of the canonical attention mechanism when processing long sequences. The previous studies have demonstrated their effectiveness on various time-series datasets across multiple domains. However, they do not deal with how the locally appearing anomalous patterns (*i.e.*, abrupt changes) of time series affect the generalization capability of models.

2.2 Robustness Against Noisy Samples and Data Imbalance

As aforementioned, deep learning models perfectly classify samples even with wrong annotations (*i.e.*, noisy samples) by simply memorizing them during the training phase [27], an issue explored widely in image classification [8,28]. Similarly, the abrupt changes in time-series forecasting are generally occurred by unexpected or unknown events, making them challenging to forecast correctly solely based on the previous time series. Due to this fact, perfectly forecasting them during the training phase indicates that the models simply memorized them which are in fact noisy samples in the time-series data.

Unlike studies addressing noisy samples in other fields, the number of abrupt changes is excessively scarce compared to that of normal states in time-series, so considering the data imbalance in addition to the noisy samples is important. The main intuition of addressing data imbalance is to emphasize the training of the minor samples based on the frequency of each class [16,26]. For example, Yang et al. [26] proposed the label distribution smoothing method that addresses the data imbalance in the image regression task. To tackle such data imbalance in time-series forecasting due to the scarce temporal patterns, few studies proposed an augmentation approach [18] or modified model architectures [10]. However, when addressing the data imbalance, they did not take account of models being

overfitted to the scarce abrupt changes during the training phase. In this regard, we propose a reweighting framework that takes both issues into account: 1) abrupt changes work as noisy samples, and 2) they cause the data imbalance.

3 Method

3.1 Preliminary

We first describe the forecasting task in a rolling window setting [15,29,25,17], which covers all possible in-output sequence pairs of the entire time series $\mathcal{S} = \{\mathbf{s}_1, \dots, \mathbf{s}_T \mid \mathbf{s}_t \in \mathbb{R}^m\}$, where T is the length of observed series and m denotes the number of variables at time t . Univariate and multivariate time-series forecasting addresses time-series data with $m = 1$ and $m > 1$, respectively. By sliding a fixed-size window on \mathcal{S} , we obtain the windows $\mathcal{D} = \{(\mathcal{X}_t, \mathcal{Y}_t)\}_{t=1}^N$, which are divided into two parts: input sequence $\mathcal{X}_t = \{\mathbf{s}_{t-I}, \dots, \mathbf{s}_{t-1}\}$ with given length I and output sequence $\mathcal{Y}_t = \{\mathbf{s}_t, \dots, \mathbf{s}_{t+O-1}\}$ with length O to predict. A forecaster f predicts the most probable length- O sequence in the future given the past length- I sequence by learning temporal dependencies in \mathcal{S} . We mainly address the loss imbalance caused by the in-output sequence pairs which include a large discrepancy between adjacent \mathcal{X}_a and \mathcal{Y}_a compared to other \mathcal{X}_t and \mathcal{Y}_t pairs where a is the time stamp with an abrupt change. However, since most time-series datasets do not provide a label for the abrupt change, we propose a training framework in an unsupervised setting.

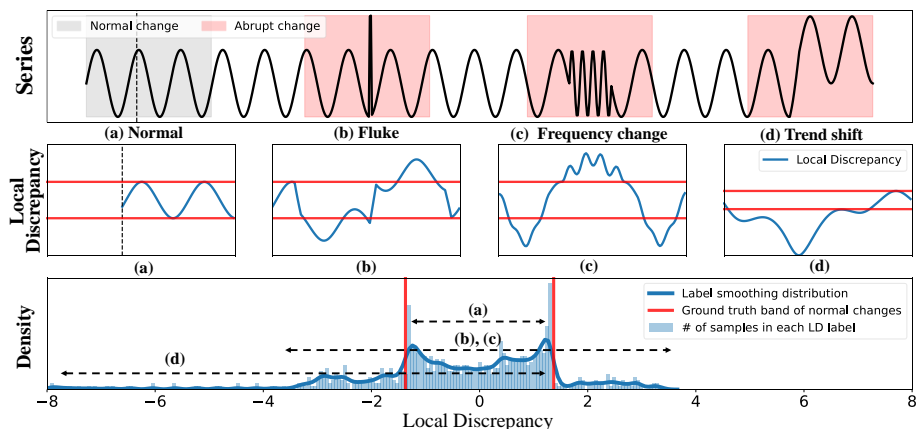


Fig. 3. The four examples of temporal changes locally seen in time series data: (a) normal, (b) fluke, (c) frequency change, and (d) trend shift. Local discrepancy computed by the sliding window captures the three abrupt changes beyond the bounds (red line) seen in normal states. In the estimated LD density distribution, training samples with abrupt changes are visibly fewer than training samples with normal state and are sparsely distributed with large absolute local discrepancy.

3.2 Local Discrepancy

We propose the *Local Discrepancy* (LD) based on a statistical difference in order to measure how two adjacent in-output sequences, \mathcal{X}_t and \mathcal{Y}_t , are different from each other. We define LD as follows:

$$\text{LocalDis}(\mathcal{X}_t, \mathcal{Y}_t) = \frac{\bar{\mathcal{X}}_t - \bar{\mathcal{Y}}_t}{\sqrt{\frac{s_{\bar{\mathcal{X}}_t}^2}{I} + \frac{s_{\bar{\mathcal{Y}}_t}^2}{O} + \varepsilon}} := v_t, \quad (1)$$

where $\bar{\mathcal{X}}_t$ is the sample mean and $s_{\bar{\mathcal{X}}_t}$ is the sample standard deviation of \mathcal{X}_t .

Statistical tests are generally used to determine whether means of two samples (*i.e.*, groups of data points in a sequence) are identical or not [24]. In this regard, we leverage t-statistic¹, a scalar value, as normalized discrepancy to measure how much two adjacent groups of samples are distinct. Figure 3 describes how LD reflects the different types of local temporal changes in time-series data (e.g., (a) normal changes, (b) fluke point, (c) frequency change, and (d) trend shift). The LD values of normal states oscillate within a certain range (see (a) red line) since the LD also has periodicity as proven by Theorem 1, but the LD values of abrupt changes is beyond the range of normal LD. Additionally, the periodicity and boundedness of LD in normal periodic series are theoretically discussed in Supplementary A with all proofs.

Theorem 1 (Periodicity of LD). *If f is a periodic function that satisfies $f(t) = f(t + p)$,*

$$LD(a, a + L) = \frac{m(a) - m(a + L)}{\sqrt{\frac{s(a)}{N} + \frac{s(a+L)}{N}}} \quad (2)$$

is also a periodic function with period p , where $m(a) = \frac{1}{N} \sum_{t \in I(a)} f(t)$, $s(a) = \frac{1}{N} \sum_{t \in I(a)} (f(t) - m(a))^2$, and $I(a) = \{a + \frac{L}{N} \cdot i\}_{i=0}^{N-1}$ for range $[a, a + L]$ and sampling interval L/N .

As aforementioned, the definition of abrupt change may be vague depending on perspectives. Thus, rather than bisecting the time stamps into abrupt changes and normal states, we utilize LD values as weights of reweighting framework to mitigate the impact of abrupt changes in training phase. In other words, losses of training samples which have large absolute v_t values will be down-weighted since we consider them to be close to the abrupt change. By computing LD over the training dataset \mathcal{D}_{train} and each of m dimensions, we obtain the dataset $\mathcal{D}_{train} = \{(\mathcal{X}_t, \mathcal{Y}_t, v_t)\}_{t=1}^N$ containing local discrepancy $v_t \in \mathbb{R}^m$ for prediction time t and for each of m dimensions. We then assign the weight $w_t = \frac{c}{|v_t|+1} \propto \frac{1}{|v_t|+1} \in \mathbb{R}^m$ to each training sample inversely to LD value of sample in \mathcal{D}_{train}

¹ Other statistics such as KPSS and t -squared can be used as LD. However, when we conduct a preliminary experiment, the t -statistic measures better than others. We further discuss the details in Section 5.

with constant c as scaling factor. Finally, we calculate the reweighted MSE loss \mathcal{L}_w as follows:

$$\mathcal{L}_w(\mathcal{Y}_t, \hat{\mathcal{Y}}_t) = \frac{1}{m \cdot O} \cdot \sum_{j=1}^m w_t^j \sum_{i=0}^{O-1} \cdot (s_{t+i}^j - \hat{s}_{t+i}^j)^2 \quad (3)$$

where $\hat{\mathcal{Y}}_t$ is forecasting results of f conditioned on \mathcal{X}_t . Through this simple reweighting framework which assigns weight inversely to LD values, namely *invLD*, we down-weight the loss of abrupt changes (large absolute LD) and up-weight the loss of normal states (small absolute LD), following the observation that the original MSE loss in the presence of abrupt changes is much larger than the loss at the normal state. Reweighting MSE only based on LD, however, does not take into account the property that normal states frequently appear while the abrupt changes are rarely included in the time-series data. We further improve our reweighting framework by considering such frequency differences between abrupt changes and normal states.

3.3 Density-based reweighting for Time-series Forecasting

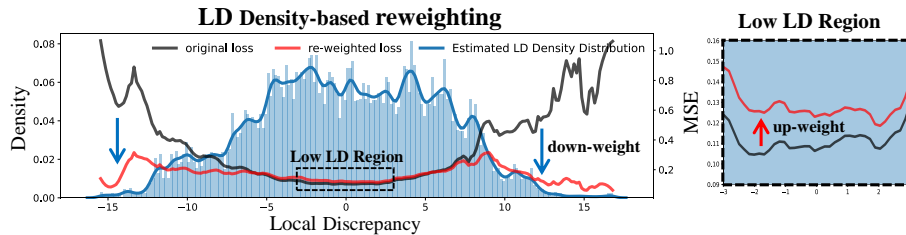


Fig. 4. For the real-world dataset (ETTh1), we visualize the estimated LD density distribution and the averaged MSE loss of samples in each LD bin after training a forecaster for one epoch. Our density-based re-weighting framework effectively down-weights (blue arrow) the losses on abrupt changes (low density and large LD) and up-weights (red arrow) those on normal states (high density and small LD).

Time series often exhibit both short-term and long-term repeating patterns [14] by periodicity, and taking them into account is crucial for making accurate predictions. Suppose a time series which has large shifts in a short period, but repeated. We can assume such large shifts are part of the normal states considering their frequent occurrences. However, this temporal pattern is down-weighted because of their large LD values regardless of the number of occurrences. In other words, *invLD* based on the inverse of LD (*i.e.*, $w_t \propto \frac{1}{|v_t|}$) will not only down-weight the loss values of abrupt changes but also those of normal states, which the model should learn to properly forecast. Therefore, we improve the time-series forecasting by considering the frequency of temporal changes (*i.e.*, LD density) when reweighting loss values in time-series forecasting.

Inspired by deep imbalanced regression [26], we use the kernel density estimation to address the missing regions between continuous LD spaces. Through

the estimated density of LD $\tilde{p}(v)$, we assign the weight $w_t = c \cdot \tilde{p}(v_t) \propto \tilde{p}(v_t)$ and use these weights to train a model as \mathcal{L}_w described in Equation 3. Figure 4 demonstrates that our final reweighting framework based on LD density, ReLD, mitigates the imbalanced loss problem in a real-world dataset. The procedure of our framework is described in Algorithm 2.

Algorithm 1 ReLD: Reweighting framework based on Local Discrepancy Density

Require: Training set $\mathcal{D} = \{(\mathcal{X}_t, \mathcal{Y}_t)\}_{t=1}^N$, bin size Δb , symmetric kernel distribution $k(v, v')$

$$\text{Compute Local Discrepancy LD } (\mathcal{X}_t, \mathcal{Y}_t) = \frac{\bar{\mathcal{X}}_t - \bar{\mathcal{Y}}_t}{\sqrt{\frac{s_{\mathcal{X}_t}^2}{T} + \frac{s_{\mathcal{Y}_t}^2}{O} + \epsilon}} := v_t$$

Compute the empirical label density distribution $p(v)$ based on Δb and \mathcal{D}

Compute the effective label density distribution $\tilde{p}(v') := \int_{\mathcal{V}} k(v, v') p(v) dv$

for all $(\mathcal{X}_t, \mathcal{Y}_t, v_t) \in \mathcal{D}$ **do**

Assign weight for each sample as $w_t \propto c \cdot \tilde{p}(v_t)$ (constant c as scaling factor)

end for

for all number of training iterations **do**

Sample a mini-batch $\{(\mathcal{X}_b, \mathcal{Y}_b, w_b)\}_{b=1}^B$ from \mathcal{D}

Forward $\{\mathcal{X}_b\}_{b=1}^B$ and get corresponding predictions $\{\hat{\mathcal{Y}}_b\}_{b=1}^B$

Do one training step using the weighted loss $\frac{1}{B} \sum_{b=1}^B \mathcal{L}_{w_b}(\hat{\mathcal{Y}}_b, \mathcal{Y}_b)$

end for

4 Experiments

This section demonstrates that our proposed framework consistently improves existing time-series forecasting models regardless of the architectures. Dataset analysis shows that our proposed framework brings larger performance gains as the number of abrupt changes in a given dataset increases. We also provide other experiments in the Supplementary, which include results on synthetic series, computational cost of methods, qualitative results, and details for reproducibility.

4.1 Experiment Setting

Dataset descriptions As mainstream benchmarks, ETT are widely used to evaluate long-term forecasting methods [29,25,17,30] ETT contains the crucial indicators (e.g., oil temperature, load, etc) collected from the electricity transformers over two years, and are categorized into four datasets depending on the location (ETT1 and ETT2) and interval (15 minutes and one hour). Electricity dataset contains the hourly electricity consumption of 321 customers from 2012 to 2014. Weather dataset is recorded every 10 minutes for a year, which contains 21 meteorological indicators (e.g., air temperature, humidity, etc). Pump dataset is collected from 52 sensors monitoring the water pump. AirQuality dataset [6], taken from the UCI repository, contains hourly averaged responses obtained from

five metal oxide chemical sensors of an chemical multi-sensor. All dataset sources can be found in Supplementary.

Forecasting models We applied it to 12 forecasting models and reported the reduced forecasting errors by applying ReLD. The baselines are roughly categorized into three groups: Transformer-based [30,17,25,29,12,15,22], CNN-based [4], and RNN-based [3,14] models. We also include two univariate forecasting models: DeepAR [20] and N-BEATS [19].

Table 1. Multivariate results with different input length I and prediction lengths O . A lower MSE indicates a better prediction and the best results in each row are bolded. Imp. means averaged MSE reduction rate for a given model and dataset. Total denotes the averaged MSE reduction rate of a given dataset across all baselines models. The full results, which include other ETT datasets and confidence interval, are available in Supplementary F.

	Models I / O	FEDformer	Pyraformer	Autoformer	Informer	Reformer	LSTNet	LSTMa	TCN	Total
		base ReLD	base ReLD	base ReLD	base ReLD	base ReLD	base ReLD	base ReLD	base ReLD	
ETTM1	96/96	0.359 0.357	0.536 0.471	0.524 0.455	0.640 0.543	0.777 0.641	0.548 0.536	0.705 0.592	0.676 0.594	-12.91%
	336/168	0.385 0.379	0.563 0.506	0.534 0.500	1.224 0.751	0.840 0.689	0.632 0.577	0.871 0.648	0.938 0.913	
	336/336	0.403 0.396	0.697 0.573	0.561 0.514	1.390 1.008	0.987 0.895	0.798 0.686	1.125 0.681	1.148 1.126	
	336/720	0.501 0.480	0.904 0.682	0.560 0.528	1.333 1.078	1.122 1.003	0.925 0.817	0.978 0.828	1.277 1.238	
	Imp.	-1.99%	-16.17%	-8.42%	-25.11%	-13.88%	-9.16%	-24.14%	-4.95%	
ETTM2	96/96	0.189 0.184	0.371 0.248	0.293 0.221	0.445 0.286	0.743 0.449	0.443 0.343	0.381 0.280	0.554 0.384	-21.42%
	336/168	0.343 0.275	0.566 0.551	0.309 0.283	2.283 1.453	1.208 0.836	0.950 0.830	1.178 0.601	1.868 1.956	
	336/336	0.338 0.315	1.601 1.330	0.508 0.331	2.479 1.764	2.239 1.425	1.610 1.019	1.479 0.745	2.769 2.773	
	336/720	0.432 0.393	5.476 5.037	0.502 0.413	6.580 5.777	3.068 2.827	6.130 4.449	3.083 2.381	3.204 3.187	
	Imp.	-9.47%	-15.15%	-21.39%	-28.29%	-28.65%	-24.85%	-36.96%	-6.57%	
Weather-h	48/48	0.338 0.336	0.292 0.279	0.344 0.343	0.345 0.294	0.343 0.313	0.318 0.310	0.346 0.325	0.348 0.327	-4.41%
	48/96	0.403 0.400	0.393 0.358	0.464 0.446	0.453 0.443	0.526 0.416	0.414 0.386	0.409 0.387	0.450 0.424	
	96/192	0.458 0.447	0.421 0.398	0.516 0.491	0.530 0.498	0.659 0.673	0.464 0.461	0.420 0.416	1.018 1.005	
	168/336	0.510 0.516	0.454 0.440	0.612 0.566	0.592 0.568	0.841 0.782	0.490 0.473	0.473 0.452	1.147 1.209	
	Imp.	-0.65%	-5.55%	-4.21%	-6.79%	-8.66%	-3.41%	-4.17%	-1.88%	
AirQuality	96/96	0.825 0.817	1.121 1.112	0.992 0.986	1.353 1.193	1.210 1.196	1.146 1.141	1.145 1.081	1.026 0.992	-3.97%
	336/168	0.811 0.808	1.193 1.115	0.911 0.922	1.796 1.595	1.473 1.345	1.231 1.156	1.644 1.376	1.246 1.163	
	336/336	0.892 0.872	1.224 1.214	0.962 0.933	1.758 1.706	1.473 1.396	1.399 1.388	1.352 1.206	1.301 1.284	
	336/720	0.997 0.953	2.196 1.982	1.129 1.079	2.914 2.985	1.723 1.671	1.826 1.921	2.475 2.333	1.442 1.426	
	Imp.	-2.01%	-4.47%	-1.72%	-5.87%	-4.51%	-0.52%	-9.63%	-3.09%	
Pump	96/96	0.520 0.513	0.848 0.796	0.558 0.538	0.831 0.870	0.826 0.760	1.016 1.007	0.813 0.766	1.037 0.970	-7.74%
	336/168	0.550 0.536	0.851 0.843	0.597 0.581	1.705 1.527	1.094 0.856	1.327 1.202	0.909 0.816	1.109 1.077	
	336/336	0.593 0.564	0.922 0.951	0.661 0.621	1.676 1.492	0.966 0.918	1.654 1.292	0.934 0.859	1.521 1.208	
	336/720	0.723 0.580	1.370 1.283	0.707 0.619	1.704 1.699	1.328 1.218	1.608 1.642	1.464 1.244	2.075 1.546	
	Imp.	-7.10%	-2.61%	-6.17%	-4.28%	-10.73%	-7.49%	-9.77%	-13.85%	

4.2 Main Results

As shown in Table 1, applying our reweighting framework reduces the MSE consistently in all existing time-series forecasting models across different datasets and varying length-averaged settings. In addition, the lowest MSE in each setting was generally achieved by the models which applied ReLD. We also observe that the performance improvements vary depending on the datasets. For example,

applying ReLD to the baselines achieves an average of 21.14% lower MSE compared to the average of original errors on ETTm2. On the other hand, applying ReLD achieves only 3.97% lower MSE on average with AirQuality dataset. We analyze such an issue in Section 4.4. As for the univariate² setting, similar to the results observed in multivariate datasets, applying ReLD enhances the forecasting performance consistently regardless of the model architectures compared to baselines without ReLD.

4.3 Comparisons with other methods

Smoothing and outlier filtering methods Table 2 (a) compares our ReLD with two smoothing and outlier filtering methods. Moving average (MA) and exponential MA (EMA) are widely used smoothing techniques that remove noisiness and reduce values of outliers, allowing meaningful temporal patterns to stand out. Similarly, outlier filtering also mitigates the influence of outliers on learning the normal patterns. However, we observe that adopting such methods either shows insignificant performance improvement or rather aggravates the time-series forecasting performance.

Error-aware loss We also compare our method with error-based reweighting approaches for robust regression (L1, Huber [11], and IRLS [5]) and data imbalance (Focal-R [16,26] and flip Focal-R). Focal-R, the regression version of focal loss, allows a model to focus on samples with relatively large loss while down-weighting loss on samples with small errors. It works in a way that is contrary to our findings. We modified such an approach by putting negation on the input of Focal-R, termed as flip Focal-R (Details in Supplementary C.2). Table 2 (b) shows that the performance of Focal-R is rather degraded while that of flip Focal-R improved. Such a result well demonstrates that our intuition, de-emphasizing the samples with high loss, is valid. Also, we observe that utilizing other error-based approaches fails to outperform our proposed method. We conjecture such superior performance of ReLD is mainly due to reflecting the temporal changes and periodicity.

Ablation study of our reweighting framework We conduct the ablation study of our proposed method by comparing our full framework ReLD and an approach which considers the LD values only (invLD). Table 2 (c) shows that our full framework is superior to invLD. Additionally, we observe that both approaches outperform the methods in (a) and (b).

4.4 Dataset Analysis

Preserving the robustness on the abrupt changes Since we impose less emphasis on the abrupt changes during the training phase, utilizing our framework may limit the model’s ability to cope with the abrupt changes in the test phase. Table 3 reports the MSE of test samples by categorizing them into time series with abrupt changes and those without abrupt changes. For the experiment, we generated synthetic time-series dataset and injected abrupt changes into the series since the real-world dataset does not have labels for abrupt changes. As originally intended, applying our framework achieves larger

² Due to space limit, the univariate result are shown in Supplementary

Table 2. Comparison with other methods which can deal with abrupt changes. We conduct experiments using ETTm2 dataset on two recent state-of-the-art time-forecasting models. ‘ \leftrightarrow ’ indicates adopting the method in replace of the original L2 loss and ‘+’ indicates adding the method to the original L2 loss.

Group	Models	FEDformer						Autoformer						Imp.
		I→O		336 → 336		336 → 720		336 → 168		336 → 336		336 → 720		
	MSE	MAE	MSE	MAE	MSE	MAE	MSE	MAE	MSE	MAE	MSE	MAE		
	Vanilla (L2)	0.343	0.406	0.338	0.387	0.432	0.461	0.309	0.371	0.508	0.490	0.502	0.478	-
(a)	+ MA	0.355	0.411	0.343	0.388	0.418	0.443	0.313	0.374	0.431	0.447	0.542	0.500	-0.85%
	+ EMA	0.364	0.419	0.343	0.389	0.404	0.432	0.319	0.377	0.516	0.473	0.549	0.506	1.33%
	+ Outlier	0.292	0.364	0.330	0.380	0.405	0.429	0.384	0.422	0.420	0.444	0.468	0.475	-3.26%
(b)	\leftrightarrow LI	0.282	0.345	0.321	0.366	0.402	0.416	0.308	0.368	0.349	0.391	0.434	0.439	-11.24%
	\leftrightarrow Huber	0.285	0.353	0.322	0.369	0.418	0.432	0.307	0.369	0.398	0.424	0.452	0.456	-8.32%
	\leftrightarrow IRLS	0.281	0.345	0.322	0.368	0.398	0.416	0.292	0.356	0.350	0.387	0.435	0.433	-12.12%
	\leftrightarrow Focal-R	0.403	0.451	0.377	0.423	0.504	0.523	0.315	0.379	0.445	0.463	0.520	0.497	6.02%
	\leftrightarrow flip Focal-R	0.284	0.344	0.322	0.367	0.405	0.417	0.307	0.366	0.371	0.405	0.470	0.453	-9.70%
(c)	+ invLD	0.282	0.343	0.326	0.374	0.402	0.414	0.288	0.353	0.343	0.385	0.411	0.421	-12.82%
	+ ReLD	0.275	0.339	0.315	0.361	0.393	0.409	0.283	0.348	0.331	0.377	0.413	0.422	-14.34%

MSE reduction rates (*i.e.*, MSE_N) compared to the ones without ReLD. As for the MSE of abrupt changes (*i.e.*, MSE_A), the MSE_A of three models decreased, and those of Pyraformer show competitive forecasting results. This result shows that our ReLD improves the forecasting performance on normal samples while preserving the robustness on the abrupt changes.

Table 3. Forecasting results by categorizing time-series sequences into normal states and abrupt changes. We observe that our ReLD significantly reduces MSE on normal states (MSE_N) while also showing comparable MSE on abrupt changes (MSE_A).

Prediction length	48		96		168		336		720		Averaged Imp.		
	Model	Metric	Base	ReLD	Base	ReLD	Base	ReLD	Base	ReLD	Base	ReLD	Total
Pyraformer	MSE_N	0.0702	0.0305	0.0580	0.0232	0.0547	0.0221	0.0449	0.0326	0.0379	0.0247	-47.67%	-27.38%
	MSE_A	0.4289	0.4168	0.5525	0.5905	0.6093	0.5882	0.4300	0.4350	0.2555	0.2665	1.21%	
Autoformer	MSE_N	0.2063	0.1473	0.2560	0.1430	0.2137	0.1261	0.3645	0.1857	0.5099	0.3950	-37.06%	-33.25%
	MSE_A	0.7385	0.6946	0.9878	0.7312	0.8152	0.6541	0.8185	0.6224	0.8230	0.6776	-18.66%	
N-BEATS	MSE_N	0.0472	0.0345	0.0592	0.0401	0.0469	0.0355	0.0646	0.0411	0.0517	0.0394	-28.73%	-17.84%
	MSE_A	0.3331	0.3794	0.6109	0.5375	0.5989	0.5944	0.4597	0.4197	0.2853	0.2909	-1.12%	
Informor	MSE_N	0.1350	0.0538	0.0819	0.0341	0.0762	0.0344	0.2954	0.0492	0.5564	0.1775	-64.96%	-51.84%
	MSE_A	0.5547	0.4746	0.5625	0.6031	0.6011	0.5810	0.7533	0.4694	0.7724	0.3619	-20.28%	

Different performance gains across datasets From the multivariate results (Table 1) and univariate results, we found that the reduction rates of MSE vary depending on the datasets. For an in-depth analysis, we present the correlation between the average of reduction rate and the average of LD for each dataset using the scatter plot in Figure 5. We observed that there exists a positive linear correlation between LD and the reduction rate, indicating that we obtain a higher reduction rate of MSE as the average of LD increases in a given dataset. To further demonstrate such a finding, we intentionally inject abrupt changes

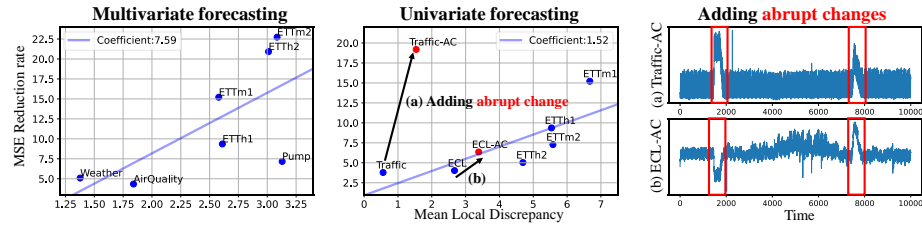


Fig. 5. Scatter plots showing the correlation between the averaged LD of each dataset and MSE reduction rates of experiments on the multivariate and univariate settings.

into the Traffic and ECL, the datasets which showed the marginal improvements in the univariate setting. We obtained a larger reduction rate of MSE with both Traffic and ECL including intentional abrupt changes compared to the original datasets. This demonstrates that the marginal performance gain in both Traffic and ECL is due to the few number of abrupt changes in the dataset. Note that datasets without such abrupt changes might be well estimated with existing time-series forecasting models. However, we emphasize that using ReLD does not degrade performance on such datasets, if not marginally improve it, due to a few number of abrupt changes inevitably included in time-series datasets.

4.5 Computational cost of ReLD

Our reweighting framework requires a marginal amount of additional computational cost of calculating the weights for all input-output sequences before training. As shown in Table 4, the cost of calculating the weights on datasets with multiple settings is less than 1% of the time it takes to train with the dataset during one epoch. The absolute time was mostly less than 1 second.

Table 4. The processing time of ReLD and training time of Autoformer during 1 epoch.

Dataset	# of Windows	Window size (I + O)	# of Series	ReLD Preprocessing time (a) (seconds)	Training time (b) (seconds per epoch)	Ratio (a) / (a) + (b)
ETTh1	8449	192 (96 + 96)	7	0.18	38.12	0.47%
ETTh2	8449	192 (96 + 96)	7	0.17	39.11	0.43%
ETTh1	34369	192 (96 + 96)	7	0.69	154.68	0.44%
ETTh2	34369	192 (96 + 96)	7	0.68	160.31	0.42%
Weather-hour	5093	1056 (336 + 720)	21	0.63	121.19	0.52%
Pump	9610	672 (336 + 336)	35	1.22	125.30	0.96%
ECL	17741	672 (336 + 336)	1	0.08	94.67	0.08%
Traffic	11225	1056 (336 + 720)	1	0.07	99.05	0.07%

5 Discussion & Limitation

In this paper, we reveal that abrupt changes between adjacent sequences deteriorate the generalization performance of time-series forecasting models by

occupying most of the losses despite their scarce occurrence in the training set. To solve this problem, we propose a simple yet effective reweighting framework that down-weights loss values of abrupt changes and up-weights those of normal states based on LD density. Although our ReLD consistently enhances the performance on real-world datasets, there is a limitation we found. We assume that an abrupt change is caused by unobserved external variables. However, if we can have access to those variables, our framework may not show performance improvement from the down-weighted losses of the abrupt changes.

References

1. Ahmad, A.S., Hassan, M.Y., Abdullah, M.P., Rahman, H.A., Hussin, F., Abdullah, H., Saidur, R.: A review on applications of ann and svm for building electrical energy consumption forecasting. *Renewable and Sustainable Energy Reviews* **33**, 102–109 (2014)
2. Anderson, O.: *Time-series*. 2nd edn. (1976)
3. Bahdanau, D., Cho, K., Bengio, Y.: Neural machine translation by jointly learning to align and translate. *arXiv preprint arXiv:1409.0473* (2014)
4. Bai, S., Kolter, J.Z., Koltun, V.: An empirical evaluation of generic convolutional and recurrent networks for sequence modeling. *arXiv preprint arXiv:1803.01271* (2018)
5. Daubechies, I., DeVore, R., Fornasier, M., Güntürk, C.S.: Iteratively reweighted least squares minimization for sparse recovery. *Communications on Pure and Applied Mathematics: A Journal Issued by the Courant Institute of Mathematical Sciences* **63**(1), 1–38 (2010)
6. De Vito, S., Massera, E., Piga, M., Martinotto, L., Di Francia, G.: On field calibration of an electronic nose for benzene estimation in an urban pollution monitoring scenario. *Sensors and Actuators B: Chemical* **129**(2), 750–757 (2008)
7. Granger, C.W.J., Newbold, P.: *Forecasting economic time series*. Academic Press (2014)
8. Han, B., Yao, Q., Yu, X., Niu, G., Xu, M., Hu, W., Tsang, I., Sugiyama, M.: Co-teaching: Robust training of deep neural networks with extremely noisy labels. In: *Proc. the Advances in Neural Information Processing Systems (NeurIPS)*. pp. 8535–8545 (2018)
9. Hotelling, H.: The generalization of student’s ratio. In: *Breakthroughs in statistics*, pp. 54–65. Springer (1992)
10. Hou, C., Wu, J., Cao, B., Fan, J.: A deep-learning prediction model for imbalanced time series data forecasting. *Big Data Mining and Analytics* **4**(4), 266–278 (2021)
11. Huber, P.J.: Robust estimation of a location parameter. In: *Breakthroughs in statistics*, pp. 492–518. Springer (1992)
12. Kitaev, N., Kaiser, L., Levskaya, A.: Reformer: The efficient transformer. In: *Proc. the International Conference on Learning Representations (ICLR)* (2019)
13. Kwiatkowski, D., Phillips, P.C., Schmidt, P., Shin, Y.: Testing the null hypothesis of stationarity against the alternative of a unit root: How sure are we that economic time series have a unit root? *Journal of econometrics* **54**(1-3), 159–178 (1992)
14. Lai, G., Chang, W.C., Yang, Y., Liu, H.: Modeling long-and short-term temporal patterns with deep neural networks. In: *The 41st International ACM SIGIR Conference on Research & Development in Information Retrieval*. pp. 95–104 (2018)

15. Li, S., Jin, X., Xuan, Y., Zhou, X., Chen, W., Wang, Y.X., Yan, X.: Enhancing the locality and breaking the memory bottleneck of transformer on time series forecasting. In: Proc. the Advances in Neural Information Processing Systems (NeurIPS) (2019)
16. Lin, T.Y., Goyal, P., Girshick, R.B., He, K., Dollár, P.: Focal loss for dense object detection. 2017 IEEE International Conference on Computer Vision (ICCV) pp. 2999–3007 (2017)
17. Liu, S., Yu, H., Liao, C., Li, J., Lin, W., Liu, A.X., Dustdar, S.: Pyraformer: Low-complexity pyramidal attention for long-range time series modeling and forecasting. In: Proc. the International Conference on Learning Representations (ICLR) (2022)
18. Moniz, N., Branco, P., Torgo, L.: Resampling strategies for imbalanced time series forecasting. *International Journal of Data Science and Analytics* **3**(3), 161–181 (2017)
19. Oreshkin, B.N., Carpov, D., Chapados, N., Bengio, Y.: N-beats: Neural basis expansion analysis for interpretable time series forecasting. In: Proc. the International Conference on Learning Representations (ICLR) (2019)
20. Salinas, D., Flunkert, V., Gasthaus, J., Januschowski, T.: Deepar: Probabilistic forecasting with autoregressive recurrent networks. *International Journal of Forecasting* **36**(3), 1181–1191 (2020)
21. Salman, A.G., Kanigoro, B., Heryadi, Y.: Weather forecasting using deep learning techniques. In: 2015 international conference on advanced computer science and information systems (ICACSIS). pp. 281–285. Ieee (2015)
22. Vaswani, A., Shazeer, N., Parmar, N., Uszkoreit, J., Jones, L., Gomez, A.N., Kaiser, Ł., Polosukhin, I.: Attention is all you need. In: Proc. the Advances in Neural Information Processing Systems (NeurIPS) (2017)
23. Vlahogianni, E.I., Karlaftis, M.G., Golias, J.C.: Short-term traffic forecasting: Where we are and where we’re going. *Transportation Research Part C: Emerging Technologies* **43**, 3–19 (2014)
24. Welch, B.L.: The significance of the difference between two means when the population variances are unequal. *Biometrika* **29**(3/4), 350–362 (1938)
25. Wu, H., Xu, J., Wang, J., Long, M.: Autoformer: Decomposition transformers with auto-correlation for long-term series forecasting. In: Proc. the Advances in Neural Information Processing Systems (NeurIPS) (2021)
26. Yang, Y., Zha, K., Chen, Y.C., Wang, H., Katabi, D.: Delving into deep imbalanced regression. In: Proc. the International Conference on Machine Learning (ICML) (2021)
27. Zhang, C., Bengio, S., Hardt, M., Recht, B., Vinyals, O.: Understanding deep learning requires rethinking generalization (2016), <http://arxiv.org/abs/1611.03530>
28. Zhang, Z., Sabuncu, M.: Generalized cross entropy loss for training deep neural networks with noisy labels. In: Proc. the Advances in Neural Information Processing Systems (NeurIPS) (2018)
29. Zhou, H., Zhang, S., Peng, J., Zhang, S., Li, J., Xiong, H., Zhang, W.: Informer: Beyond efficient transformer for long sequence time-series forecasting. In: Proc. the AAAI Conference on Artificial Intelligence (AAAI) (2021)
30. Zhou, T., Ma, Z., Wen, Q., Wang, X., Sun, L., Jin, R.: Fedformer: Frequency enhanced decomposed transformer for long-term series forecasting. In: Proc. the International Conference on Machine Learning (ICML) (2022)

A Theoretical analysis of ReLD

As shown in Figure 3 of main paper, we can observe LD values oscillating within a certain range similarly to original time series. We discuss the following points about this observation.

1. When the time series is sampled from a periodic function, LD is also a periodic function.
2. When the time series is sampled from a bounded periodic function, LD is bounded.

First, we can easily prove that LD is also periodic when the time series is sampled from a periodic function, which the model should learn from data (i.e., normal states).

Theorem 1. If f is a periodic function that satisfies $f(t) = f(t + p)$,

$$LD(a, a + L) = \frac{m(a) - m(a + L)}{\sqrt{\frac{s(a)}{N} + \frac{s(a+L)}{N}}} \quad (4)$$

is also a periodic function with period p , where $m(a) = \frac{1}{N} \sum_{t \in I(a)} f(t)$, $s(a) = \frac{1}{N} \sum_{t \in I(a)} (f(t) - m(a))^2$, and $I(a) = \{a + \frac{L}{N} \cdot i\}_{i=0}^{N-1}$ for range $[a, a + L]$ and sampling interval L/N .

To prove Theorem 1, we prove and use Proposition 1 and 2 with respect to the mean and the variance of the periodic function.

Proposition 1. If f is a periodic function that satisfies $f(t) = f(t + p)$, $m(a) = \frac{1}{N} \sum_{t \in I(a)} f(t)$ is also a periodic function with period p where $I(a) = \{a + \frac{L}{N} \cdot i\}_{i=0}^{N-1}$ for range $[a, a + L]$ and sampling interval L/N .

Proposition 2. If f is a periodic function that satisfies $f(t) = f(t + p)$, $s(a) = \frac{1}{N} \sum_{x \in I(a)} (f(t) - m(a))^2$ is also a periodic function with period p where $I(a) = \{a + \frac{L}{N} \cdot i\}_{i=0}^{N-1}$ for range $[a, a + L]$ and sampling interval L/N .

By proposition 1 and 2, we prove Theorem 1 as follows:

$$\begin{aligned} LD(a + p, a + p + L) &= \frac{m(a + p) - m(a + p + L)}{\sqrt{\frac{s(a+p)}{N} + \frac{s(a+p+L)}{N}}} \\ &= \frac{m(a) - m(a + L)}{\sqrt{\frac{s(a)}{N} + \frac{s(a+L)}{N}}} \\ &= LD(a, a + L) \end{aligned}$$

Regarding the bound of LD, if we define LD by ignoring the variances (i.e., $LD(a, a + L) = m(a) - m(a + L)$), we can obtain the bound $2 \cdot B$ given that f is bounded function that satisfies $|f(t)| \leq B$ for all t .

However, since we use the variance of input and output, LD can diverge when both variances of input sequence and output sequence are equal to zero. There are two cases when the variance equals to zero.

1. f is a constant function.
2. The window size L is $N \cdot p$ for data points, which are sampled from a periodic function f with the period p and sampling interval L/N .

In the first case, since the time-series dataset has a constant target value, the prediction also remains as the constant value, leading to a trivial solution. In the second case, the variance is no longer zero if the window size L is adjusted.

In practice, we use epsilon ϵ as a numerical stabilizer to solve the case where variances are zero as shown in Equation 1. Note that we do not use these bounds as thresholds in the proposed method.

Proofs for the Proposition 1 and 2 are as follows.

Proposition 1. If f is periodic function that satisfy $f(t) = f(t + p)$, $m(a) = \frac{1}{N} \sum_{t \in I(a)} f(t)$ is also periodic function with period p where $I(a) = \{a + \frac{L}{N} \cdot i\}_{i=0}^{N-1}$ for range $[a, a + L]$ and sampling interval L/N .

Proof:

$$\begin{aligned}
 m(a + p) &= \frac{1}{N} \sum_{t \in I(a+p)} f(t) \\
 &= \frac{1}{N} \left\{ f(a + p) + f\left(a + p + \frac{L}{N}\right) + \cdots + f\left(a + p + L - \frac{L}{N}\right) \right\} \\
 &= \frac{1}{N} \left\{ f(a) + f\left(a + \frac{L}{N}\right) + \cdots + f\left(a + L - \frac{L}{N}\right) \right\} \\
 &= m(a)
 \end{aligned}$$

Proposition 2. If f is periodic function that satisfy $f(t) = f(t + p)$, $s(a) = \frac{1}{N} \sum_{t \in I(a)} (f(t) - m(a))^2$ is also periodic function with period p where $I(a) = \{a + \frac{L}{N} \cdot i\}_{i=0}^{N-1}$ for range $[a, a + L]$ and sampling interval L/N .

Proof:

$$\begin{aligned}
 s(a + p) &= \frac{1}{N} \sum_{t \in I(a+p)} \{f(t) - m(a + p)\}^2 \\
 &= \frac{1}{N} \left\{ (f(a + p) - m(a + p))^2 + \left(f\left(a + p + \frac{L}{N}\right) - m(a + p)\right)^2 \right. \\
 &\quad \left. + \cdots + \left(f\left(a + p + L - \frac{L}{N}\right) - m(a + p)\right)^2 \right\} \\
 &= \frac{1}{N} \left\{ (f(a) - m(a))^2 + \left(f\left(a + \frac{L}{N}\right) - m(a)\right)^2 + \cdots + \left(f\left(a + L - \frac{L}{N}\right) - m(a)\right)^2 \right\} \\
 &= s(a)
 \end{aligned}$$

B In-Depth Analysis on ReLD

This section provides various analysis for our reweighting framework.

B.1 Abrupt change with external variables

We assumed that an abrupt change can be caused by unobserved and external events as we mentioned in Section 1 and Section 5. If the abrupt change can be predicted using an external variable, down-weighting the loss of the abrupt change would get in the way of learning such correlation for the model. However, utilizing additional variables without thorough verification causes the model to learn a spurious correlation between variables, which worsens the generalization ability. Moreover, some abrupt changes have unknown causes (e.g., sensor malfunction), which cannot be addressed by simply collecting external variables. In fact, as shown in the Table 5, we observed that training baseline models with external variables (i.e., Multivariate to Univariate denoted as Mul2Uni setting) rather shows lower performance than training those with the target time series only (i.e., Univariate to Univariate denoted as Uni2Uni setting). These results indicate that simply adding covariates does not guarantee performance gains. Note that multivariate forecasting we mentioned in main paper is multivariate to multivariate setting (i.e., Mul2Mul), which is different with Mul2Uni setting. In addition, applying our method on Mul2Uni outperformed the Uni2Uni in several cases (see Autoformer 96/96 and 336/168 of Table 5).

Table 5. Comparison between Mul2Uni and Uni2Uni forecasting on ETTm1 dataset.

Model	Pyraformer			Autoformer		
	96 → 96	336 → 168	336 → 336	96 → 96	336 → 168	336 → 336
Uni2Uni	0.0821 ± 0.0289	0.1286 ± 0.0346	0.1941 ± 0.0523	0.0577 ± 0.0081	0.0881 ± 0.0284	0.0903 ± 0.0096
Uni2Uni + Ours	0.0576 ± 0.0079	0.1218 ± 0.0395	0.1843 ± 0.0507	0.0522 ± 0.0035	0.0723 ± 0.0068	0.0847 ± 0.0084
Mul2Uni	0.1757 ± 0.0372	0.2926 ± 0.0778	0.5920 ± 0.0591	0.0619 ± 0.0090	0.0799 ± 0.0188	0.1367 ± 0.0392
Mul2Uni + Ours	0.1137 ± 0.0295	0.2984 ± 0.1246	0.5533 ± 0.0761	0.0496 ± 0.0021	0.0674 ± 0.0071	0.1193 ± 0.0267

B.2 ReLD on repeated changes

To further understand our ReLD, we present a rectangular time series as a special case, which generally includes a large shift during a short period of time and shows increasing amplitude (see 1st row of Figure 6). Although this series includes large shifts, we do not regard those as abrupt changes defined in our paper since rectangular patterns are repeated (i.e., seasonal component). Also, the increasing amplitude (i.e., trend component) is considered one of the trend types. Since we calculate LD by sliding the window, the increasing amplitude does not change the LD values. For example, the LD value of the window, which of size is large enough to cover period, has a value less than 0 (greater than 0 if

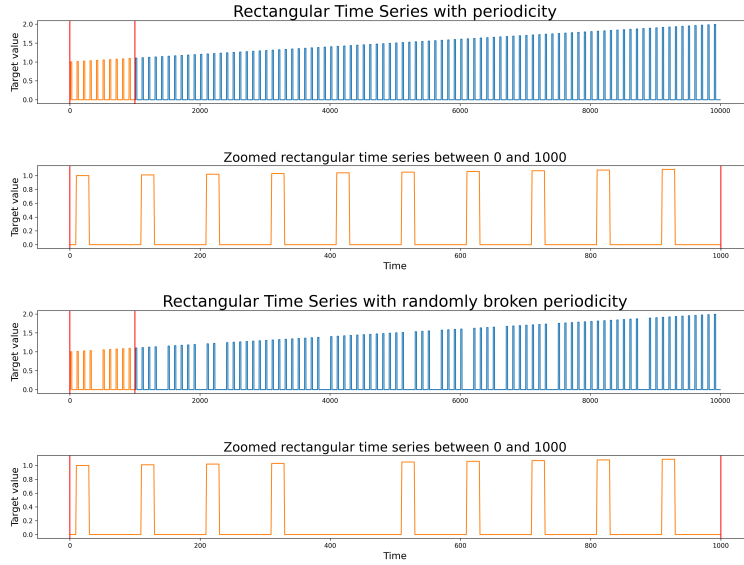


Fig. 6. Two rectangular time series which include large shift in a short time. As in the first row, if a rectangular pattern with a large change exists several times, ReLD learns it normally without down-weighting it. However, if the periodicity is broken by sensor malfunctions in the third row, ReLD mitigates impact of anomaly pattern in training phase.

the amplitude decreases) regardless of time. In this case, since the LD values of all windows are similar, they will be given the same weights. Therefore, even if our method is applied, we would observe more or less the same performance as shown in Rect-Normal dataset of Table 6. Additionally, we conducted experiments by removing rectangles randomly from the dataset (see 3rd row of Figure 6). This can be considered abrupt changes (e.g., broken periodicity). We observe that our ReLD brings performance gain in such cases (see Rect-Broken of Table 6). This again demonstrates that our proposed method promotes the model to be robust to abrupt changes.

B.3 Impact of the in-output ratio

We conducted an experiment by fixing the output length and changing the input length from 48 to 720 to explore the performance change according to the I/O ratio. We conducted experiments on the three datasets, ETTh1, ETTh2, and ETTm1. Applying our method brings consistent performance improvements, although there exists different performance gains depending on the input lengths as shown in Table 7.

Table 6. Rectangular Time Series with the increasing amplitude and the randomly broken periodicity.

Models		Pyraformer		Autoformer		Informer	
MSE		base	our	base	our	base	our
Rect-Normal	96	0.2405 ± 0.0211	0.2468 ± 0.0243	0.9748 ± 0.4805	0.9131 ± 0.4100	0.5409 ± 0.0280	0.5480 ± 0.0316
	168	0.2614 ± 0.0115	0.2652 ± 0.0102	1.4711 ± 0.9902	1.7147 ± 0.7723	1.3573 ± 0.1377	1.3556 ± 0.1068
	336	0.3179 ± 0.0075	0.3193 ± 0.0062	0.5271 ± 0.2047	0.4492 ± 0.1558	1.2945 ± 0.0874	1.2764 ± 0.0891
	720	0.4034 ± 0.0084	0.4088 ± 0.0089	2.7076 ± 0.4390	2.6447 ± 0.6276	1.6796 ± 0.0450	1.7306 ± 0.0614
Imp.		1.46%		-1.72%		0.71%	
Rect-Broken	96	0.4028 ± 0.0434	0.2343 ± 0.0061	0.9883 ± 0.1790	1.1399 ± 0.4871	0.5781 ± 0.0558	0.3912 ± 0.0463
	168	0.3261 ± 0.0138	0.3020 ± 0.0174	1.7361 ± 0.8130	1.2914 ± 0.3595	0.5622 ± 0.0386	0.5227 ± 0.0178
	336	0.2548 ± 0.0112	0.2579 ± 0.0155	0.7678 ± 0.1225	0.5648 ± 0.1603	0.5144 ± 0.0394	0.4988 ± 0.0494
	720	0.3098 ± 0.0617	0.3037 ± 0.0427	2.0861 ± 0.1504	1.8670 ± 0.3713	0.5936 ± 0.0473	0.5569 ± 0.0390
Imp.		-12.49%		-11.80%		-12.14%	

Table 7. Impact of the ratio I/O on multivariate time series forecasting.

Models		Pyraformer		Autoformer		Informer		Imp.
Output-96	Input	base	our	base	our	base	our	
ETTh1	48	0.6314 ± 0.0371	0.5166 ± 0.0104	0.4748 ± 0.0328	0.4675 ± 0.0504	1.0632 ± 0.2707	0.8125 ± 0.0679	-23.58%
	96	0.6453 ± 0.0583	0.5345 ± 0.0073	0.4531 ± 0.0282	0.4452 ± 0.0153	0.9075 ± 0.0479	0.8476 ± 0.0532	-6.6%
	168	0.6330 ± 0.0241	0.5604 ± 0.0145	0.4477 ± 0.0247	0.4594 ± 0.0426	0.8997 ± 0.0738	0.7928 ± 0.0698	-11.88%
	336	0.7195 ± 0.0206	0.6310 ± 0.0293	0.4667 ± 0.0240	0.4826 ± 0.0188	1.1695 ± 0.2012	1.0384 ± 0.1830	-11.21%
	720	0.7290 ± 0.0757	0.6540 ± 0.0191	0.6354 ± 0.0386	0.5057 ± 0.0673	1.6608 ± 0.1402	1.3866 ± 0.1341	-16.51%
ETTh2	48	1.5411 ± 0.1880	1.0982 ± 0.1702	0.3637 ± 0.0091	0.3394 ± 0.0051	1.7225 ± 0.1508	1.1461 ± 0.0743	-22.96%
	96	1.6090 ± 0.0866	1.1733 ± 0.2271	0.3731 ± 0.0294	0.3464 ± 0.0102	3.4245 ± 0.4814	2.4505 ± 0.4804	-20.89%
	168	1.7787 ± 0.2003	1.3081 ± 0.2461	0.4414 ± 0.0271	0.3833 ± 0.0069	5.6370 ± 0.8005	2.9705 ± 0.4835	-28.97%
	336	1.7924 ± 0.2872	1.5560 ± 0.1676	0.4897 ± 0.0565	0.4174 ± 0.0517	6.2992 ± 0.9310	3.9496 ± 0.8050	-21.75%
	720	2.0959 ± 0.1960	1.9368 ± 0.2612	0.6769 ± 0.1552	0.4701 ± 0.0869	9.1387 ± 2.0638	6.9792 ± 1.5690	-20.59%
ETTm1	48	0.5559 ± 0.0225	0.4922 ± 0.0134	0.5673 ± 0.0542	0.5182 ± 0.0396	0.6389 ± 0.0270	0.5925 ± 0.0348	-9.13%
	96	0.5364 ± 0.0318	0.4713 ± 0.0299	0.5128 ± 0.0635	0.4545 ± 0.0410	0.6438 ± 0.0596	0.5367 ± 0.0439	-13.38%
	168	0.5015 ± 0.0431	0.4174 ± 0.0176	0.4987 ± 0.0241	0.4603 ± 0.0636	0.6907 ± 0.0578	0.5677 ± 0.0281	-14.09%
	336	0.4876 ± 0.0325	0.4316 ± 0.0171	0.5374 ± 0.0361	0.5053 ± 0.0462	0.8487 ± 0.0578	0.6078 ± 0.0541	-15.28%
	720	0.4841 ± 0.0381	0.4546 ± 0.0224	0.5799 ± 0.0914	0.4988 ± 0.0384	1.0951 ± 0.1741	0.8007 ± 0.1602	-15.65%

C Comparison with other methods

C.1 Comparison with smoothing and outlier filtering

We compared our proposed method with 1) smoothing and 2) outlier filtering which are expected to perform well with drastic changes (e.g., fluke) in time-series datasets. Smoothing techniques are used to remove nosiness and reduce outliers, allowing meaningful temporal patterns to stand out. Conventional methods include moving average (MA) smoothing as follows:

$$s_t = \frac{(x_{t-k+1} + x_{t-k+2} + \dots + x_t)}{k} \quad (5)$$

where s_t is the smoothed observation at t and x_t is the original observation. The other method is exponential (EMA) smoothing calculated by Equation as follows:

$$s_t = \alpha \cdot x_t + (1 - \alpha) \cdot s_{t-1} \quad (6)$$

where $\alpha \in (0, 1)$. We smoothed the training time series and train forecasting models. To use outlier filtering method for forecasting task, a simple way to detect outliers is to assume that the target value follows a Gaussian and remove values that exceed a certain range of values. We train forecasters after removing outliers which exceed a certain value.

C.2 Comparison with error-based reweighting

As we mentioned in the main paper, we observed that abrupt changes significantly contribute to the total loss in the training phase. In this situation, we can simply reweight a loss of sample that have large error while considering the sample including abrupt change. Reweighting inversely to the error may down-weight the loss of the abrupt change without additional LD calculation. In the main paper, we presented two error-based methods: Focal-R and flip Focal-R. Focal-R loss is calculated as $\sigma(\beta |e_i|)^\gamma L_i$ where e_i is error of i -th sample, L_i is loss of i -th sample, and $\sigma(\cdot)$ is sigmoid function. β and γ are hyperparameters. In case of flip Focal-R, β is negative to flip the sigmoid function along the y axis. Additionally, we provide L2 error-based reweighting results, namely invL2 which is written as $\frac{L_i}{e_i + \epsilon}$. In case of invL2, as the model forecasts accurately and thus the error of the normal states is close to zero, the parameter moves with larger steps by up-weighted loss. Table 8 shows the performance in the case of reweighting inversely to the error of each window.

C.3 Variants for Local Discrepancy

We propose the *Local Discrepancy* (LD) based on the statistics formulated by a statistical test, Welch’s t-test [24], in order to measure how two adjacent in-output sequences, \mathcal{X}_t and \mathcal{Y}_t , are different from each other. There may exist other metrics to measure the local discrepancy such as multivariate t-statistic [9] (i.e., Hotelling’s t -squared statistic) and stationarity tests (e.g.,

Table 8. Comparison with error-based reweighting (invL2) in the multivariate forecasting (Top) and in the univariate forecasting (Bottom) using ETTh1 dataset.

Multivariate I / O	Pyraformer			Autoformer			Informer		
	base	invL2	ReLD	base	invL2	ReLD	base	invL2	ReLD
96 / 96	0.6453 ± 0.0583	0.6083 ± 0.0149	0.5345 ± 0.0073	0.4422 ± 0.0242	0.4458 ± 0.0212	0.4438 ± 0.0143	0.9084 ± 0.0485	0.8506 ± 0.0280	0.8031 ± 0.0317
336 / 168	0.8644 ± 0.0905	0.7842 ± 0.0250	0.7415 ± 0.0399	0.5042 ± 0.0515	0.4772 ± 0.0144	0.4906 ± 0.0263	1.3720 ± 0.2422	1.2150 ± 0.1333	0.8858 ± 0.0258
336 / 336	0.9328 ± 0.0341	0.9643 ± 0.0404	0.8895 ± 0.0548	0.5694 ± 0.1115	0.5450 ± 0.0886	0.5110 ± 0.0990	1.3425 ± 0.0725	1.2857 ± 0.0710	0.9850 ± 0.0308
336 / 720	0.9843 ± 0.0213	1.0003 ± 0.0228	0.9781 ± 0.0196	0.5348 ± 0.0212	0.5589 ± 0.0613	0.5207 ± 0.0106	1.3933 ± 0.0892	1.3735 ± 0.0386	1.1994 ± 0.0597
Imp.	-	-2.50%	-9.17%	-	-1.08%	-3.81%	-	-5.86%	-21.89%

Univariate I / O	Pyraformer			Autoformer			Informer		
	base	invL2	ReLD	base	invL2	ReLD	base	invL2	ReLD
96 / 96	0.2074 ± 0.0728	0.1928 ± 0.0365	0.1831 ± 0.0533	0.0859 ± 0.0063	0.0861 ± 0.0031	0.0841 ± 0.0067	0.1203 ± 0.0730	0.1132 ± 0.0441	0.1020 ± 0.0472
336 / 168	0.1819 ± 0.0257	0.1750 ± 0.0581	0.1725 ± 0.0406	0.1077 ± 0.0130	0.0949 ± 0.0109	0.0999 ± 0.0072	0.0862 ± 0.0292	0.0946 ± 0.0244	0.0848 ± 0.0297
336 / 336	0.1716 ± 0.0597	0.1853 ± 0.0622	0.1649 ± 0.0426	0.1055 ± 0.0219	0.1135 ± 0.0198	0.1008 ± 0.0157	0.0862 ± 0.0025	0.0870 ± 0.0084	0.0897 ± 0.0165
336 / 720	0.1974 ± 0.0415	0.1746 ± 0.0312	0.1667 ± 0.0298	0.1352 ± 0.0207	0.1251 ± 0.0110	0.1244 ± 0.0270	0.2025 ± 0.0961	0.1800 ± 0.0945	0.1550 ± 0.0237
Imp.	-	-3.60%	-9.09%	-	-2.88%	-5.45%	-	-1.59%	-9.06%

Kwiatkowski–Phillips–Schmidt–Shin (KPSS) tests [13]). We also report the performance of our reweighting framework using a different metric other than t -statistics for measuring the local discrepancy in Table 9. Hotelling’s t -squared statistic is a generalization of Student’s t -statistic that is used in multivariate hypothesis testing. We can naturally utilize t -squared statistic as LD for multivariate forecasting (*i.e.*, $\mathbf{s} \in \mathbb{R}^m$ and $m > 1$) as follows:

$$\text{LocalDis}(\mathcal{X}_t, \mathcal{Y}_t) = \frac{I \cdot O}{I + O} (\bar{\mathcal{X}}_t - \bar{\mathcal{Y}}_t)' \hat{\Sigma}^{-1} (\bar{\mathcal{X}}_t - \bar{\mathcal{Y}}_t) := v_t^2 \quad (7)$$

where the mean and covariance are defined as follows:

$$\bar{\mathcal{X}}_t = \frac{1}{I} \sum_{i=1}^I \mathbf{s}_{t-i}, \quad \bar{\mathcal{Y}}_t = \frac{1}{O} \sum_{i=0}^{O-1} \mathbf{s}_{t+i}, \quad \hat{\Sigma} = \frac{(I-1) \hat{\Sigma}_{\bar{\mathcal{X}}} + (O-1) \hat{\Sigma}_{\bar{\mathcal{Y}}}}{I+O-2},$$

$$\hat{\Sigma}_{\bar{\mathcal{X}}} = \frac{1}{I-1} \sum_{i=1}^I (\mathbf{s}_{t-i} - \bar{\mathcal{X}}_t) (\mathbf{s}_{t-i} - \bar{\mathcal{X}}_t)', \quad \hat{\Sigma}_{\bar{\mathcal{Y}}} = \frac{1}{O-1} \sum_{i=1}^{O-1} (\mathbf{s}_{t+i} - \bar{\mathcal{Y}}) (\mathbf{s}_{t+i} - \bar{\mathcal{Y}})'.$$

We can interpret the time-series data in terms of stochastic processes. KPSS tests are used for testing a null hypothesis that an observable time series is stationary around a deterministic trend (*i.e.*, trend-stationary) against the alternative of a unit root. When the given time series is trend stationary, the KPSS statistic has small value, which is close to zero. Thus, to measure the degree of abruptness of a change in a given period of time, we leverage the KPSS statistic as LD:

$$\text{LocalDis}(\text{concat}(\mathcal{X}_t, \mathcal{Y}_t)) = \frac{1}{(I+O)^2} \cdot \sum_{i=-I}^{O-1} \frac{\mathcal{E}_{t+i}^2}{\hat{\sigma}^2} := v_t \quad (8)$$

where \mathcal{E}_t is partial sum of the residuals and $\hat{\sigma}^2$ is the estimate of the long-run variance of the residuals as follows:

$$\mathcal{E}_k = \sum_{i=1}^k e_i, \quad e = (e_{t-I}, e_{t-I+1}, \dots, e_{O-1})$$

where e means OLS residuals when regressing the concated in-output sequence (*i.e.*, $\text{concat}(\mathcal{X}_t, \mathcal{Y}_t)$). We observe that our reweighting framework consistently

Table 9. Ablation study on variants of local discrepancy used in our reweighting framework. We compare models which uses 1) KPSS, 2) t -squared, and 3) t -statistic. The t -statistic shows more consistent and superior results compared to other statistics in the multivariate setting.

Dataset		ETTh1			ETTh2			ETTm1			Imp.
Model	Predict-O	96	168	336	96	168	336	96	168	336	
Pyraformer		0.645	0.864	0.933	1.609	5.014	4.356	0.536	0.563	0.697	-
Pyraformer + KPSS		0.554	0.782	0.909	1.482	4.590	5.327	0.470	0.527	0.604	-5.84%
Pyraformer + t -squared		0.640	0.809	0.898	1.440	3.112	3.912	0.490	0.557	0.632	-9.84%
Pyraformer + t -statistic		0.534	0.742	0.889	1.173	3.976	3.281	0.471	0.506	0.573	-16.51%
Autoformer		0.442	0.504	0.569	0.386	0.439	0.494	0.524	0.534	0.561	-
Autoformer + KPSS		0.446	0.528	0.486	0.358	0.436	0.516	0.456	0.538	0.513	-3.68%
Autoformer + t -squared		0.454	0.521	0.515	0.357	0.403	0.436	0.503	0.548	0.512	-4.60%
Autoformer + t -statistic		0.444	0.491	0.511	0.351	0.413	0.424	0.455	0.500	0.514	-7.74%
Informer		0.908	1.372	1.343	3.400	5.796	3.901	0.640	1.224	1.390	-
Informer + KPSS		0.850	1.215	1.215	3.050	5.593	4.202	0.535	0.844	1.087	-11.41%
Informer + t -squared		0.871	1.262	1.234	2.796	4.393	3.419	0.594	0.992	1.195	-12.76%
Informer + t -statistic		0.856	1.113	1.151	2.462	4.723	3.788	0.543	0.751	1.008	-18.81%

outperforms the ones without our framework regardless of the statistics used for measuring the local discrepancy. While we empirically confirmed that using t -statistic is more suitable for LD compared to KPSS or t -Squared statistic, such result demonstrates that our framework can be used with any statistics measure the user deems appropriate.

D Our Framework Details

D.1 Implementation details

We include 12 baselines to validate our ReLD. All models were implemented with PyTorch. As for recent models (*i.e.*, FEDformer³, Pyraformer⁴, Autoformer⁵, and Informer⁶), we used the official code released by the original authors, rather than implementing from scratch. For a fair comparison between ReLD and the existing framework, we set the same hyperparameters found in each work. We trained all models from scratch to 10 epochs. To assign weights to all training samples in ReLD, the LD is computed only once before training, and it takes only

³ <https://github.com/MAZiqing/FEDformer>

⁴ <https://github.com/alipay/Pyraformer>

⁵ <https://github.com/thuml/Autoformer>

⁶ <https://github.com/zhouhaoyi/Informer2020>

a negligible amount of time compared to the training time. Most models, which leverage a generative decoding, take an average of less than an hour to train on a TITAN-Xp GPU except for LSTMa which uses auto-regressive decoding.

D.2 Dataset details

In this work, we reported the results on eight datasets. ETT are widely used to evaluate long-term forecasting methods [29,25,17,30] ETT contains the crucial indicators (e.g., oil temperature, load, etc) collected from the electricity transformers over two years, and are categorized into four datasets depending on the location (ETT1 and ETT2) and interval (15 minutes and one hour). Electricity ⁷ dataset contains the hourly electricity consumption of 321 customers from 2012 to 2014. Weather dataset ⁸ is recorded every 10 minutes for a year, which contains 21 meteorological indicators (e.g., air temperature, humidity, etc). Pump dataset ⁹ is collected from 52 sensors monitoring the water pump. AirQuality dataset ¹⁰, taken from the UCI repository, contains hourly averaged responses obtained from five metal oxide chemical sensors of an air quality chemical multi-sensor device.

D.3 Pseudo code for ReLD

Algorithm 2 ReLD: Reweighting framework based on Local Discrepancy Density

Require: Training set $\mathcal{D} = \{(\mathcal{X}_t, \mathcal{Y}_t)\}_{t=1}^N$, bin size Δb , symmetric kernel distribution $k(v, v')$

Compute Local Discrepancy LD $(\mathcal{X}_t, \mathcal{Y}_t) = \frac{\bar{\mathcal{X}}_t - \bar{\mathcal{Y}}_t}{\sqrt{\frac{s_{\mathcal{X}_t}^2}{T} + \frac{s_{\mathcal{Y}_t}^2}{O} + \epsilon}} := v_t$

Compute the empirical label density distribution $p(v)$ based on Δb and \mathcal{D}
 Compute the effective label density distribution $\tilde{p}(v') := \int_{\mathcal{V}} k(v, v') p(v) dv$

for all $(\mathcal{X}_t, \mathcal{Y}_t, v_t) \in \mathcal{D}$ **do**

 Assign weight for each sample as $w_t \propto c \cdot \tilde{p}(v_t)$ (constant c as scaling factor)

end for

for all number of training iterations **do**

 Sample a mini-batch $\{(\mathcal{X}_b, \mathcal{Y}_b, w_b)\}_{b=1}^B$ from \mathcal{D}

 Forward $\{\mathcal{X}_b\}_{b=1}^B$ and get corresponding predictions $\{\hat{\mathcal{Y}}_b\}_{b=1}^B$

 Do one training step using the weighted loss $\frac{1}{B} \sum_{b=1}^B \mathcal{L}_{w_b}(\hat{\mathcal{Y}}_b, \mathcal{Y}_b)$

end for

We illustrate the pseudo code of the ReLD in Algorithm 2.

⁷ <https://archive.ics.uci.edu/ml/datasets/ElectricityLoadDiagrams20112014>

⁸ <https://www.bgc-jena.mpg.de/wetter/>

⁹ <https://www.kaggle.com/datasets/nphantawee/pump-sensor-data>

¹⁰ <https://archive.ics.uci.edu/ml/datasets/air+quality>

D.4 Hyperparameter Sensitivity

We used KDE to smooth the LD distribution. Related parameters include the bin size that determines how many sections continuous LD is divided into, KDE’s kernel type, kernel size and kernel sigma. In our experiment, we set the bin size to 200, kernel type to Gaussian, and kernel size and sigma to 5 and 2, respectively, as default parameters. We conducted experiments on ETTh1 and ETTh2 to observe the variance of performance according to each parameter. As shown in Table 11, Table 12, Table 13, and Table 14, we observe that our proposed method is robust to the hyper-parameters while showing consistent performance improvements.

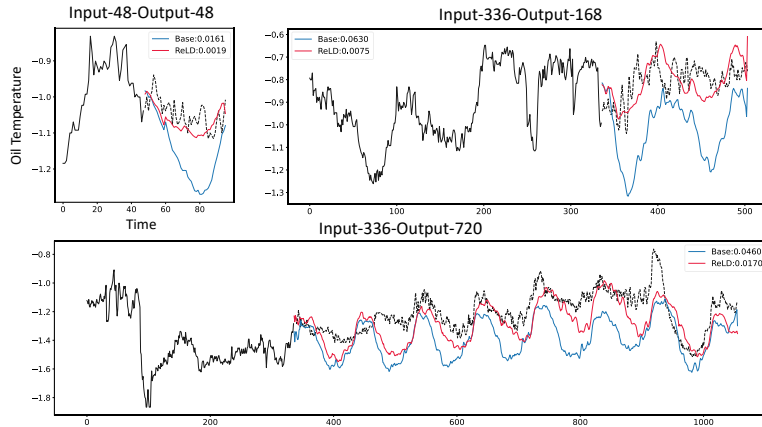


Fig. 7. Forecasting results of Autoformer trained on ETTm1 with three different length settings: Input-48-Output-48, Input-336-Output-168, and Input-336-Output-720. The blue line indicates the forecasting results of the baselines without our ReLD and the red line indicates those with our ReLD.

E Qualitative Results

This section visualizes the forecasting results using three criteria: in-output length (Figure 7), dataset (Figure 8), and model architecture (Figure 9). All samples are from the test set of each dataset. The solid black line denotes the input series and the dotted black line denotes the ground truth series that a model should predict. For a reliable comparison, we plot the averaged forecasting results of the independent models trained from different random initializations. The shaded part of the forecasting result indicates the forecasting variation at a given time stamp. In Figure 7, we only report the mean of forecasting results without the forecasting variation for better clarity.

Table 10. Performance change according to the number of bins.

Dataset		ETTh1	ETTh2	
Model	# bins	336 → 336	96 → 96	Imp.
Autoformer	-	0.5694 ± 0.1115	0.3859 ± 0.0260	-
Autoformer + ReLD	40	0.5245 ± 0.1543	0.3529 ± 0.0262	-8.55%
	120	0.4907 ± 0.0337	0.3455 ± 0.0229	-10.47%
	200	0.4903 ± 0.0610	0.3501 ± 0.0168	-9.28%
	300	0.4881 ± 0.0413	0.3472 ± 0.0072	-10.03%
	500	0.5130 ± 0.0529	0.3485 ± 0.0142	-9.69%

Table 11. Performance change according to the KDE kernel types.

Dataset		ETTh1	ETTh2	
Model	KDE kernel	336 → 336	96 → 96	Imp.
Autoformer	-	0.5694 ± 0.1115	0.3859 ± 0.0260	-
Autoformer + ReLD	Gaussian	0.4903 ± 0.0610	0.3501 ± 0.0168	-9.28%
	Triangle	0.4792 ± 0.0171	0.3453 ± 0.0232	-10.52%
	Laplace	0.4786 ± 0.0380	0.3496 ± 0.0087	-9.41%

Table 12. Performance changes according to the KDE kernel size.

Dataset		ETTh1	ETTh2	
Model	KDE kernel size	336 → 336	96 → 96	Imp.
Autoformer	-	0.5694 ± 0.1115	0.3859 ± 0.0260	-
Autoformer + ReLD	5	0.4903 ± 0.0610	0.3501 ± 0.0168	-9.28%
	10	0.4896 ± 0.0728	0.3466 ± 0.0018	-10.18%
	15	0.4836 ± 0.0189	0.3567 ± 0.0293	-7.57%
	20	0.4841 ± 0.0444	0.3482 ± 0.0383	-9.77%
	25	0.4835 ± 0.0317	0.3490 ± 0.0166	-9.56%

Table 13. Performance change according to the KDE kernel sigma.

Dataset		ETTh1	ETTh2	
Model	KDE kernel sigma	336 → 336	96 → 96	Imp.
Autoformer	-	0.5694 ± 0.1115	0.3859 ± 0.0260	-
Autoformer + ReLD	1	0.5545 ± 0.1916	0.3521 ± 0.0189	-8.76%
	2	0.4903 ± 0.0610	0.3501 ± 0.0168	-9.28%
	4	0.5218 ± 0.1632	0.3586 ± 0.0567	-7.07%
	8	0.4767 ± 0.0307	0.3435 ± 0.0172	-10.99%
	16	0.4836 ± 0.0318	0.3494 ± 0.0310	-9.46%

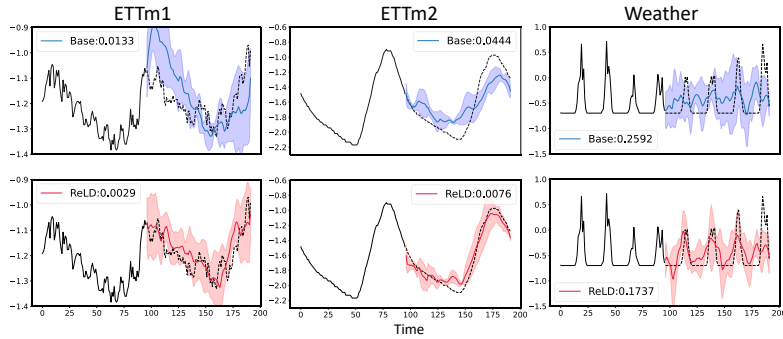


Fig. 8. Forecasting results of Autoformer on three datasets: ETTm1, ETTm2, and Weather. The first row shows the forecasting results of the baseline without our ReLD and the second row shows those with our ReLD.

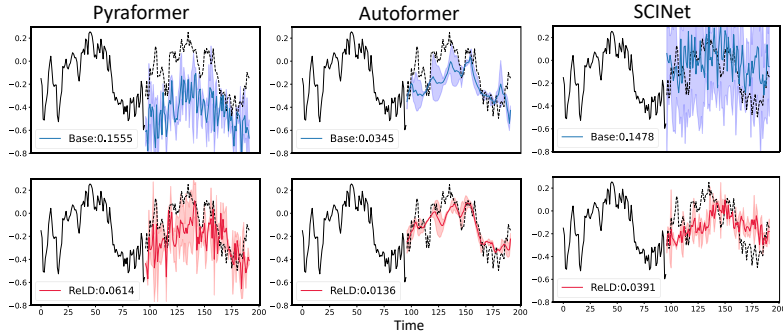


Fig. 9. Forecasting results of the recent three models on the same sample in HULL series of ETTm2. The first row shows the forecasting results of the baselines without our ReLD and the second row shows those with our ReLD.

As shown in Figure 7, our ReLD demonstrated enhanced forecasting results in both short-term and long-term settings. We observe that applying ReLD significantly reduces the MSE loss regardless of datasets (see Figure 8) and model architectures (Figure 9). For example, by applying ReLD on Weather dataset (see Figure 8), the prediction variations (red-shaded regions) are fitted to the fluctuations of the target times series which was underfitted without applying ReLD (blue-shaded regions).

F Full Benchmark on the Real-World Datasets

Models	FEDformer		Pyraformer		Autoformer		Informer		Log/Trans		Reformer		Transformer		LSTNet		LSTMa		TCN			
	base	our	base	our	base	our	base	our	base	our	base	our	base	our	base	our	base	our	base	our		
ETTm1	MSE	0.3479	0.3483	0.5354	0.4438	0.4160	0.3842	0.6872	0.5734	0.7247	0.5902	0.7393	0.6409	0.6615	0.5443	0.6272	0.5586	0.6938	0.5809	0.5655	0.4862	
	48	± 0.0017	± 0.0017	± 0.0157	± 0.0139	± 0.0216	± 0.0181	± 0.0736	± 0.0409	± 0.0764	± 0.0473	± 0.0260	± 0.0173	± 0.0767	± 0.0370	± 0.0115	± 0.0069	± 0.0447	± 0.0334	± 0.0287	± 0.0151	
	96	0.3774	0.3743	0.6453	0.4422	0.4438	0.9084	0.8561	0.6584	0.5772	0.8031	0.7306	0.8652	0.7160	0.7605	0.6816	0.8290	0.6613	0.7628	0.6794	0.6794	
	168	± 0.0018	± 0.0016	± 0.0584	± 0.0074	± 0.0243	± 0.0143	± 0.0486	± 0.0522	± 0.0574	± 0.0307	± 0.0317	± 0.0216	± 0.1242	± 0.0289	± 0.0365	± 0.0354	± 0.1048	± 0.0551	± 0.0429	± 0.0152	
	336	0.4446	0.4367	0.8644	0.7415	0.5042	0.4906	1.3720	1.1125	1.0497	0.9355	0.8858	0.7677	1.0911	0.8628	0.9276	0.7904	1.0522	0.8622	0.9406	0.9319	
ETTm2	MSE	0.4479	0.4453	0.9328	0.8895	0.5694	0.5110	1.3425	1.1507	1.0618	0.9874	0.9850	0.8481	1.1712	1.0429	1.0125	0.9586	1.1677	0.9672	1.1093	1.1120	
	48	± 0.0075	± 0.0059	± 0.0341	± 0.0548	± 0.1115	± 0.0990	± 0.0725	± 0.0305	± 0.2052	± 0.1435	± 0.0308	± 0.0130	± 0.0721	± 0.0560	± 0.0758	± 0.0449	± 0.0875	± 0.1548	± 0.0555	± 0.0625	
	96	0.5088	0.5064	0.9843	0.9781	0.5348	0.5207	1.3933	1.3912	1.0621	1.0621	1.1995	1.1994	1.0481	1.1264	1.0834	1.1154	1.0965	1.4609	1.3927	1.1604	1.1484
	168	± 0.0131	± 0.0192	± 0.0214	± 0.0196	± 0.0213	± 0.0107	± 0.0893	± 0.0444	± 0.1705	± 0.2349	± 0.0597	± 0.0449	± 0.0765	± 0.0656	± 0.0391	± 0.1134	± 0.1274	± 0.0653	± 0.0156	± 0.0156	
	336	Imp.	-0.71%	-10.75%	-4.57%	-11.13%	-11.13%	-7.17%	-12.44%	-14.13%	-14.13%	-8.62%	-15.28%	-5.33%	Imbalance							
ETTh1	MSE	0.2539	0.2569	0.7756	0.6186	0.2984	0.2815	0.9560	0.6438	1.1329	0.6747	0.8518	0.6777	1.1950	0.6794	0.8930	0.6791	0.8816	0.5750	0.9044	0.6387	
	48	± 0.0004	± 0.0010	± 0.0910	± 0.0369	± 0.0072	± 0.0061	± 0.1512	± 0.0916	± 0.0825	± 0.1191	± 0.0350	± 0.0400	± 0.3054	± 0.0608	± 0.0805	± 0.0480	± 0.0832	± 0.0213	± 0.1185	± 0.1452	
	96	0.3420	0.3304	1.6090	1.1733	0.3859	0.3514	3.4000	2.4616	2.7501	2.1171	1.8490	1.3124	2.0744	1.7618	1.4426	1.1167	1.6695	0.9905	1.7404	1.5293	
	168	± 0.0024	± 0.0033	± 0.0866	± 0.0271	± 0.0261	± 0.0124	± 0.5346	± 0.4278	± 0.6731	± 0.3310	± 0.2863	± 0.1231	± 0.1893	± 0.3022	± 0.0179	± 0.0990	± 0.5567	± 0.1973	± 0.4478	± 0.1754	
	336	0.4021	0.3837	5.0138	3.9761	0.4394	0.4131	5.7957	4.7229	2.2557	2.2054	3.1301	2.2042	3.9472	4.0993	3.3118	2.8871	3.9065	2.5133	2.4321	2.4058	
ETTh2	MSE	0.4006	0.3842	4.3559	3.2814	0.4942	0.4239	3.9011	3.7882	4.4043	3.6032	2.9343	2.2374	2.8095	2.9328	3.9730	3.0537	2.9757	2.1797	2.9652	2.9037	
	48	± 0.0108	± 0.0071	± 0.3957	± 0.5145	± 0.0307	± 0.0338	± 0.6699	± 0.7034	± 0.5353	± 0.2468	± 0.3673	± 0.1497	± 0.5978	± 0.3583	± 0.3591	± 0.2037	± 0.4939	± 0.3570	± 0.1794	± 0.1749	
	96	0.4520	0.4429	4.2013	3.4771	0.4502	0.4209	4.0175	3.9606	2.4391	2.7142	2.6307	2.6276	2.6471	3.0069	3.7246	2.9905	3.2982	2.6797	3.1513	3.1454	
	168	± 0.0363	± 0.0315	± 0.5338	± 0.2490	± 0.0414	± 0.0232	± 0.5374	± 0.3356	± 0.2176	± 0.5075	± 0.2001	± 0.2424	± 0.5341	± 0.4458	± 0.1502	± 0.3913	± 0.4699	± 0.2820	± 0.0452	± 0.0637	
	336	Imp.	-2.58%	-21.98%	-8.26%	-16.62%	-16.62%	-14.52%	-20.58%	-7.28%	-20.44%	-31.32%	-8.99%	Electrical								
ETTh1	MSE	0.5146	0.5190	0.5632	0.5564	0.5487	0.4924	0.6332	0.5984	0.5800	0.5696	0.7703	0.7276	0.6136	0.5882	0.6415	0.6136	0.6744	0.6478	0.6768	0.6428	
	48	± 0.0091	± 0.0124	± 0.0285	± 0.0443	± 0.0865	± 0.0329	± 0.0150	± 0.0266	± 0.0225	± 0.0186	± 0.0320	± 0.0077	± 0.0164	± 0.0439	± 0.0463	± 0.0256	± 0.0253	± 0.0336	± 0.0620	± 0.0156	
	96	0.3594	0.3580	0.5364	0.4713	0.5239	0.4547	0.6404	0.5429	0.7070	0.5969	0.7773	0.6409	0.5787	0.5157	0.5484	0.5365	0.7054	0.5920	0.6758	0.5930	
	168	± 0.0035	± 0.0033	± 0.0319	± 0.0300	± 0.0851	± 0.0476	± 0.0570	± 0.0368	± 0.0470	± 0.0310	± 0.0698	± 0.0582	± 0.0672	± 0.0293	± 0.0358	± 0.0251	± 0.0793	± 0.0838	± 0.0333	± 0.0259	
	336	0.3850	0.3790	0.5631	0.5056	0.5341	0.5001	1.2238	0.7507	0.8866	0.7534	0.8398	0.6889	0.7928	0.7268	0.6323	0.5774	0.8710	0.6477	0.9382	0.9128	
ETTh2	MSE	0.0259	0.0138	0.0737	0.0346	0.0366	0.0300	0.1911	0.0776	0.1458	0.0856	0.0346	0.0220	0.0628	0.0320	0.0282	0.0378	0.0883	0.0661	0.0412	0.0288	
	48	± 0.0107	± 0.0090	± 0.0855	± 0.0707	± 0.0217	± 0.0214	± 0.1481	± 0.0877	± 0.0582	± 0.0570	± 0.0519	± 0.0184	± 0.1637	± 0.1313	± 0.1058	± 0.0390	± 0.1963	± 0.0222	± 0.0318	± 0.0696	
	96	0.4033	0.3955	0.6970	0.5729	0.5613	0.5145	1.3896	1.0085	0.9685	0.8368	0.9874	0.8946	0.9579	0.9262	0.7985	0.6858	1.1254	0.6810	1.1476	1.1258	
	168	± 0.0107	± 0.0090	± 0.0855	± 0.0707	± 0.0217	± 0.0214	± 0.1481	± 0.0877	± 0.0582	± 0.0570	± 0.0519	± 0.0184	± 0.1637	± 0.1313	± 0.1058	± 0.0390	± 0.1963	± 0.0222	± 0.0318	± 0.0696	
	336	0.5010	0.4805	0.9037	0.6822	0.5601	0.5278	1.3329	1.0780	1.1222	0.9226	1.1216	1.0027	1.0858	1.0393	0.9248	0.8168	0.9782	0.8280	1.2768	1.2351	
ETTm1	MSE	0.0456	0.0297	0.1019	0.0624	0.0578	0.0301	0.1013	0.0966	0.1009	0.0750	0.0227	0.0421	0.1066	0.0785	0.0516	0.0886	0.1870	0.1288	0.0243	0.0097	
	48	± 0.0142	± 0.0138	± 0.0286	± 0.0200	± 0.1708	± 0.1689	± 0.2953	± 0.2143	± 0.3191	± 0.2394	± 0.4635	± 0.3293	± 0.3317	± 0.2794	± 0.2923	± 0.2826	± 0.2736	± 0.2494	± 0.3619	± 0.2555	
	96	0.1886	0.1844	0.3709	0.2480	0.2934	0.2213	0.4451	0.2860	0.5480	0.3844	0.7433	0.4491	0.4636	0.2993	0.4430	0.3426	0.3807	0.2798	0.5537	0.3839	
	168	± 0.0008	± 0.0012	± 0.1396	± 0.0164	± 0.0691	± 0.0126	± 0.0519	± 0.0221	± 0.0984	± 0.0594	± 0.0230	± 0.0384	± 0.0845	± 0.0384	± 0.0899	± 0.0391	± 0.0377	± 0.0165	± 0.0965	± 0.0607	
	336	0.3429	0.2751	0.5655	0.5515	0.3095	0.2834	2.2831	1.4531	1.4953	1.1491	1.2078	0.8359	1.7806	1.3650	0.9504	0.8304	1.1780	0.6010	1.8678	1.9539	
ETTm2	MSE	0.0240	0.0021	0.0940	0.0586	0.0130	0.0086	0.1434	0.1662	0.2619	0.1603	0.1790	0.0428	0.2845	0.2038	0.0953	0.0878	0.2799	0.0853	0.1214	0.0890	
	48	± 0.0060	± 0.0016	± 0.3115	± 0.2605	± 0.1483	± 0.0158	± 0.1344	± 0.1074	± 0.4704	± 0.3334	± 0.2275	± 0.0750	± 0.2138	± 0.0497	± 0.1013	± 0.1412	± 0.1184	± 0.1485	± 0.0594	± 0.0594	
	96	0.3381	0.3151	1.6013	1.3296	0.5084	0.3313	2.4795	1.7639	3.4383	2.6429	2.2391	1.4248	1.9661	1.5664	1.6096	1.0193	1.4788	0.7454	2.7687	2.7734	
	168	± 0.0060	± 0.0016	± 0.3115	± 0.2605	± 0.1483	± 0.0158	± 0.1344	± 0.1074	± 0.4704	± 0.3334	± 0.2275	± 0.0750	± 0.2138	± 0.0497	± 0.1013	± 0.1412	± 0.1184	± 0.1485	± 0.0594	± 0.0594	
	336	0.4322	0.3930	5.4764	5.0372	5.0222	4.132	6.5797	5.7777	5.6465	6.1251	3.0679	2.8266	4.5449								

Models	FEDformer	Pyraformer	Autoforemer	Informer	LogTrans	Reformer	Transformer	LSTNet	LSTMa	TCN										
MSE	base	our	base	our	base	our	base	our	base	our										
Pump																				
48	0.5246	0.5227	0.7242	0.7151	0.5767	0.5439	0.8648	0.7334	0.7886	0.7129	0.8083	0.7282	0.8434	0.6645	0.8234	0.7343	0.7540	0.7155	0.8649	0.8310
	± 0.0024	± 0.0012	± 0.0184	± 0.0153	± 0.0364	± 0.0042	± 0.0294	± 0.1065	± 0.0569	± 0.0673	± 0.0318	± 0.0155	± 0.0664	± 0.0697	± 0.0376	± 0.0110	± 0.0238	± 0.0295	± 0.0920	± 0.0964
96	0.5197	0.5135	0.8484	0.7958	0.5576	0.5381	0.8314	0.8699	0.9948	0.9839	0.8261	0.7605	0.9108	0.8816	1.0155	1.0068	0.8126	0.7660	1.0367	0.9699
	± 0.0026	± 0.0021	± 0.0309	± 0.0284	± 0.0098	± 0.0192	± 0.0732	± 0.0987	± 0.1275	± 0.1926	± 0.0619	± 0.0332	± 0.0997	± 0.1224	± 0.1262	± 0.1170	± 0.0676	± 0.0374	± 0.1635	± 0.0383
168	0.5502	0.5363	0.8512	0.8431	0.5974	0.5814	1.7047	1.5268	1.2820	1.3845	1.0941	0.8555	1.1326	1.1846	1.3271	1.2025	0.9088	0.8161	1.1093	1.0771
	± 0.0061	± 0.0057	± 0.0470	± 0.0330	± 0.0252	± 0.0194	± 0.1863	± 0.1589	± 0.1141	± 0.2210	± 0.2337	± 0.0902	± 0.1874	± 0.1399	± 0.2779	± 0.2055	± 0.1720	± 0.0700	± 0.0529	± 0.0788
336	0.5931	0.5638	0.9225	0.9508	0.6615	0.6209	1.6763	1.4923	0.9181	0.9100	0.9658	0.9183	1.1494	1.1369	1.6537	1.2921	0.9340	0.8587	1.5206	1.2081
	± 0.0525	± 0.0109	± 0.0405	± 0.0520	± 0.0248	± 0.0144	± 0.3531	± 0.2763	± 0.0463	± 0.0816	± 0.0598	± 0.0385	± 0.3206	± 0.2823	± 0.4863	± 0.3871	± 0.1100	± 0.0966	± 0.0914	± 0.1237
720	0.7230	0.5802	1.3697	1.2829	0.7066	0.6191	1.7041	1.6986	0.9746	0.9082	1.3278	1.2181	1.5309	1.7408	1.6076	1.6421	1.4645	1.2439	2.0748	1.5455
	± 0.2988	± 0.0318	± 0.2434	± 0.1263	± 0.0144	± 0.0203	± 0.2126	± 0.0835	± 0.0806	± 0.0435	± 0.0993	± 0.0630	± 0.3202	± 0.3619	± 0.3964	± 0.1623	± 0.4705	± 0.5097	± 0.4642	± 0.1738
Imp.	-5.75%		-2.34%		-6.08%		-5.07%		-2.08%		-10.57%		-1.44%		-8.16%		-8.83%		-11.87%	
AirQuality																				
48	0.7306	0.7447	0.8780	0.8579	0.8606	0.8520	0.9094	0.8682	0.9281	0.8010	1.1148	0.9913	0.9718	0.8877	1.0227	0.9738	0.9273	0.8540	0.8829	0.8358
	± 0.0131	± 0.0254	± 0.0675	± 0.0712	± 0.0191	± 0.0425	± 0.0579	± 0.0610	± 0.1007	± 0.0443	± 0.0509	± 0.0463	± 0.0409	± 0.0707	± 0.0654	± 0.0522	± 0.1077	± 0.0242	± 0.1588	± 0.1005
96	0.8251	0.8166	1.1207	1.1122	0.9976	0.9271	1.3526	1.1934	1.0586	1.0653	1.2099	1.1961	1.1338	1.0816	1.1462	1.1413	1.1454	1.0810	1.0260	0.9915
	± 0.0025	± 0.0027	± 0.1378	± 0.1346	± 0.0667	± 0.0638	± 0.0255	± 0.0788	± 0.0867	± 0.0535	± 0.0452	± 0.0546	± 0.1105	± 0.1563	± 0.0491	± 0.0279	± 0.1172	± 0.1114	± 0.0392	± 0.0360
168	0.8108	0.8080	1.1930	1.1149	0.9141	0.9256	1.7961	1.5947	1.8682	1.9269	1.4728	1.3455	1.8278	1.7274	1.2313	1.1560	1.6440	1.3756	1.2456	1.1629
	± 0.0141	± 0.0164	± 0.1415	± 0.0557	± 0.0214	± 0.0844	± 0.1993	± 0.1155	± 0.2617	± 0.4315	± 0.1751	± 0.1253	± 0.4175	± 0.2465	± 0.0753	± 0.0128	± 0.2291	± 0.2611	± 0.0523	± 0.0954
336	0.8918	0.8724	1.2240	1.2140	0.9525	0.9295	1.7579	1.7060	1.6436	1.4867	1.4731	1.3958	1.4636	1.4199	1.3990	1.3881	1.3524	1.2055	1.3006	1.2844
	± 0.0066	± 0.0112	± 0.0475	± 0.0475	± 0.0683	± 0.0525	± 0.0597	± 0.0608	± 0.2307	± 0.1592	± 0.1082	± 0.0760	± 0.1249	± 0.0744	± 0.0595	± 0.0429	± 0.2118	± 0.1609	± 0.0564	± 0.0660
720	0.9974	0.9527	2.1962	1.9817	1.1018	1.0593	2.9136	2.9346	3.3683	2.8386	1.7234	1.6715	2.4630	2.4953	1.8259	1.9214	2.3104	2.2325	1.4419	1.4256
	± 0.0302	± 0.0261	± 0.1120	± 0.1065	± 0.0378	± 0.0508	± 0.1185	± 0.2300	± 0.3599	± 0.5806	± 0.0728	± 0.0258	± 0.1430	± 0.2564	± 0.0761	± 0.0689	± 0.2172	± 0.1665	± 0.0792	± 0.0703
Imp.	-1.22%		-4.04%		-2.62%		-5.61%		-7.04%		-5.82%		-4.09%		-1.37%		-8.82%		-3.54%	
Weather-h																				
48	0.3376	0.3357	0.2922	0.2786	0.3441	0.3425	0.3454	0.2941	0.3593	0.3262	0.3429	0.3127	0.3047	0.2860	0.3181	0.3099	0.3457	0.3245	0.3476	0.3270
	± 0.0026	± 0.0023	± 0.0047	± 0.0057	± 0.0075	± 0.0064	± 0.0149	± 0.0131	± 0.0263	± 0.0147	± 0.0227	± 0.0113	± 0.0040	± 0.0095	± 0.0078	± 0.0060	± 0.0158	± 0.0071	± 0.0133	± 0.0091
96	0.4031	0.3997	0.3933	0.3578	0.4636	0.4455	0.4528	0.4471	0.3856	0.5264	0.4163	0.4279	0.3704	0.4142	0.3857	0.4090	0.3873	0.4502	0.4243	0.4243
	± 0.0057	± 0.0198	± 0.0095	± 0.0074	± 0.0277	± 0.0215	± 0.0551	± 0.0291	± 0.0229	± 0.0217	± 0.0448	± 0.0372	± 0.0214	± 0.0118	± 0.0115	± 0.0158	± 0.0131	± 0.0416	± 0.0279	
168	0.4578	0.4466	0.4207	0.3978	0.5163	0.4907	0.5304	0.4984	0.4706	0.4431	0.6591	0.6726	0.5106	0.4813	0.4641	0.4612	0.4198	0.4164	1.0181	1.0051
	± 0.0256	± 0.0154	± 0.0160	± 0.0105	± 0.0232	± 0.0190	± 0.0582	± 0.0583	± 0.0369	± 0.0555	± 0.1473	± 0.1001	± 0.0384	± 0.0218	± 0.0388	± 0.0245	± 0.0168	± 0.0187	± 0.0500	± 0.1028
336	0.5099	0.5162	0.4540	0.4401	0.6123	0.5662	0.5921	0.5680	0.5736	0.5854	0.8411	0.7824	0.5051	0.4726	0.4905	0.4730	0.4727	0.4518	1.1468	1.2091
	± 0.0250	± 0.0197	± 0.0269	± 0.0201	± 0.0374	± 0.0339	± 0.0244	± 0.0204	± 0.11297	± 0.0899	± 0.0633	± 0.0867	± 0.0455	± 0.0457	± 0.0198	± 0.0133	± 0.0159	± 0.0212	± 0.1591	± 0.1111
Imp.	-0.65%		-5.55%		-4.21%		-6.79%		-6.69%		-8.66%		-7.94%		-3.41%		-4.17%		-1.88%	

Models	FEDformer		Pyraformer		Autoformer		N-BEATS		Informr		LogTrans		Reformer		Transformer		DeepPAR		LSTNet		TCN		
	base	our	base	our	base	our	base	our	base	our	base	our	base	our	base	our	base	our	base	our	base	our	
ETTm1	48	0.0509	0.0490	0.1485	0.1144	0.0760	0.0658	0.1337	0.0963	0.2216	0.1608	0.1257	0.1247	0.3218	0.2940	0.1925	0.1479	0.3035	0.2499	0.1294	0.1130	0.1770	0.1230
		± 0.0010	± 0.0008	± 0.0149	± 0.0079	± 0.0134	± 0.0057	± 0.0290	± 0.0230	± 0.1100	± 0.0463	± 0.0474	± 0.0249	± 0.1346	± 0.1004	± 0.1114	± 0.0983	± 0.0400	± 0.0196	± 0.0051	± 0.0030	± 0.0164	± 0.0264
	96	0.0809	0.0786	0.2074	0.1831	0.0859	0.0841	0.1203	0.1020	0.2168	0.2189	0.2164	0.1884	0.4816	0.4268	0.2266	0.1912	0.3849	0.3361	0.2322	0.2213	0.3485	0.3169
		± 0.0014	± 0.0007	± 0.0728	± 0.0533	± 0.0064	± 0.0067	± 0.0730	± 0.0472	± 0.0425	± 0.0443	± 0.1065	± 0.0804	± 0.2308	± 0.1818	± 0.0960	± 0.0881	± 0.0529	± 0.0994	± 0.0068	± 0.0112	± 0.0808	± 0.1107
	168	0.1053	0.0996	0.1819	0.1725	0.1077	0.0999	0.0862	0.0848	0.1951	0.1829	0.2206	0.2051	0.5079	0.4489	0.2471	0.2189	0.2463	0.2653	0.2641	0.2388	0.3142	0.3120
ETTm2	48	0.0069	0.0171	0.0257	0.0406	0.0131	0.0072	0.0292	0.0029	0.0514	0.0567	0.0313	0.0293	0.2215	0.1202	0.0475	0.0437	0.0177	0.0144	0.0590	0.0443	0.0449	0.0170
		± 0.0075	± 0.0035	± 0.0597	± 0.0427	± 0.0220	± 0.0157	± 0.0025	± 0.0165	± 0.0181	± 0.0483	± 0.0408	± 0.0440	± 0.1648	± 0.1152	± 0.0271	± 0.0190	± 0.0390	± 0.0333	± 0.0569	± 0.0302	± 0.0668	± 0.0472
	96	0.1531	0.1345	0.1974	0.1667	0.1352	0.1244	0.2025	0.1550	0.1562	0.1508	0.2910	0.2542	0.4813	0.4977	0.2004	0.1473	0.2764	0.2589	0.3086	0.2611	0.4077	0.4184
		± 0.0365	± 0.0224	± 0.0416	± 0.0299	± 0.0207	± 0.0237	± 0.0962	± 0.0237	± 0.0705	± 0.0676	± 0.0748	± 0.0434	± 0.0808	± 0.0904	± 0.0533	± 0.0324	± 0.0283	± 0.0291	± 0.0237	± 0.0348	± 0.0466	± 0.0376
	720	Imp.	-7.15%	-11.86%	-7.04%	-12.84%	-4.73%	-7.91%	-7.48%	-17.34%	-5.72%	-10.14%	-8.19%	-10.14%	-8.19%								
ETTm1	48	0.0924	0.0922	0.1072	0.1105	0.1294	0.1235	0.1108	0.1142	0.1466	0.1317	0.1143	0.1054	0.1775	0.1689	0.1269	0.1105	0.2587	0.2203	0.1129	0.1140	0.1148	0.1084
		± 0.0003	± 0.0003	± 0.0008	± 0.0135	± 0.0074	± 0.0070	± 0.0195	± 0.0202	± 0.0027	± 0.0067	± 0.0043	± 0.0041	± 0.0077	± 0.0054	± 0.0165	± 0.0098	± 0.0234	± 0.0175	± 0.0051	± 0.0046	± 0.0052	± 0.0140
	96	0.1282	0.1307	0.1806	0.1292	0.1533	0.1548	0.1270	0.1233	0.2690	0.2216	0.1831	0.1770	0.1978	0.1896	0.2448	0.2099	0.3225	0.2808	0.1750	0.1587	0.1658	0.1577
		± 0.0013	± 0.0012	± 0.0588	± 0.0074	± 0.0038	± 0.0073	± 0.0076	± 0.0040	± 0.1029	± 0.0364	± 0.0107	± 0.0481	± 0.0070	± 0.0047	± 0.0034	± 0.0196	± 0.0289	± 0.0056	± 0.0044	± 0.0152	± 0.0159	
	168	0.1893	0.1788	0.1708	0.1653	0.2000	0.1980	0.1782	0.1896	0.2679	0.2505	0.2358	0.2323	0.2207	0.2185	0.2556	0.2434	0.3104	0.2730	0.2080	0.2201	0.1938	0.1865
ETTm2	48	0.0170	0.0092	0.0133	0.0140	0.0096	0.0119	0.0188	0.0324	0.0164	0.0214	0.0208	0.0332	0.0054	0.0089	0.0416	0.0333	0.0599	0.0234	0.0189	0.0249	0.0177	0.0183
		± 0.0169	± 0.0184	± 0.0170	± 0.0102	± 0.0189	± 0.0091	± 0.0254	± 0.0304	± 0.0322	± 0.0140	± 0.0403	± 0.0164	± 0.0031	± 0.0142	± 0.0189	± 0.0111	± 0.0590	± 0.0534	± 0.0281	± 0.0360	± 0.0138	± 0.0163
	96	0.2069	0.1984	0.1866	0.1837	0.2140	0.2059	0.2058	0.2242	0.2776	0.2422	0.2585	0.2375	0.2059	0.2148	0.2706	0.2611	0.3558	0.3110	0.2685	0.2461	0.2060	0.2083
		± 0.0241	± 0.0098	± 0.0170	± 0.0102	± 0.0189	± 0.0091	± 0.0254	± 0.0304	± 0.0322	± 0.0140	± 0.0403	± 0.0164	± 0.0031	± 0.0142	± 0.0189	± 0.0111	± 0.0590	± 0.0534	± 0.0281	± 0.0360	± 0.0138	± 0.0163
	720	0.2545	0.2499	0.1897	0.1608	0.2789	0.2655	0.3938	0.3685	0.3098	0.2908	0.2140	0.2198	0.1869	0.1893	0.2485	0.2814	0.3029	0.3982	0.3741	0.1973	0.2107	0.2157
ETTm1	48	0.0306	0.0201	0.0371	0.0229	0.0476	0.0119	0.1487	0.1271	0.0285	0.0244	0.0081	0.0109	0.0063	0.0035	0.0227	0.0529	0.0188	0.0770	0.1034	0.0141	0.0141	0.0148
		± 0.0306	± 0.0201	± 0.0371	± 0.0229	± 0.0476	± 0.0119	± 0.1487	± 0.1271	± 0.0285	± 0.0244	± 0.0081	± 0.0109	± 0.0063	± 0.0035	± 0.0227	± 0.0529	± 0.0188	± 0.0770	± 0.1034	± 0.0141	± 0.0141	± 0.0148
	96	Imp.	-1.95%	-9.08%	-2.63%	1.81%	-10.63%	-3.60%	-0.88%	-6.29%	-8.95%	-3.38%	-3.12%	-3.38%									
		± 0.0230	± 0.0221	± 0.0288	± 0.0255	± 0.0357	± 0.0328	± 0.0306	± 0.0295	± 0.0428	± 0.0356	± 0.0375	± 0.0332	± 0.0784	± 0.0699	± 0.0315	± 0.0317	± 0.0843	± 0.0501	± 0.0304	± 0.0287	± 0.0342	± 0.0327
	168	0.0359	0.0350	0.0821	0.0576	0.0577	0.0522	0.0851	0.0659	0.1051	0.0831	0.1051	0.0582	0.2280	0.1608	0.0888	0.0596	0.1790	0.0849	0.0622	0.0512	0.0841	0.0780
ETTm2	48	0.0830	0.0662	0.1286	0.1218	0.0881	0.0723	0.0771	0.0701	0.1808	0.1576	0.1924	0.1612	0.2840	0.2227	0.2211	0.1960	0.1999	0.1985	0.1243	0.1223	0.1945	0.2159
		± 0.0283	± 0.0087	± 0.0347	± 0.0395	± 0.0284	± 0.0069	± 0.0275	± 0.0188	± 0.0400	± 0.0282	± 0.0575	± 0.0395	± 0.0309	± 0.0477	± 0.0732	± 0.0622	± 0.0350	± 0.0308	± 0.0157	± 0.0264	± 0.0436	± 0.0419
	96	0.0808	0.0758	0.1941	0.1843	0.0903	0.0847	0.1336	0.1248	0.2631	0.2273	0.3671	0.3041	0.3394	0.3039	0.2739	0.2469	0.3821	0.4323	0.2973	0.2629	0.3286	0.3106
		± 0.0046	± 0.0018	± 0.0524	± 0.0507	± 0.0085	± 0.0085	± 0.0368	± 0.0121	± 0.0558	± 0.0481	± 0.0606	± 0.0130	± 0.0227	± 0.0358	± 0.1049	± 0.0487	± 0.0783	± 0.0607	± 0.0367	± 0.0450	± 0.0352	
	720	0.1094	0.1025	0.3368	0.2753	0.1428	0.1119	0.1444	0.1118	0.3914	0.3486	0.4738	0.3805	0.3956	0.4097	0.4786	0.4426	0.4979	0.4179	0.3692	0.2937	0.4134	0.4452
ETTm2	48	0.0136	0.0253	0.0928	0.0563	0.0618	0.0270	0.0342	0.0452	0.1149	0.1133	0.0667	0.0389	0.0255	0.0291	0.0737	0.1325	0.0795	0.0847	0.0291	0.0219	0.0892	0.0889
		± 0.0136	± 0.0253	± 0.0928	± 0.0563	± 0.0618	± 0.0270	± 0.0342	± 0.0452	± 0.1149	± 0.1133	± 0.0667	± 0.0389	± 0.0255	± 0.0291	± 0.0737	± 0.1325	± 0.0795	± 0.0847	± 0.0291	± 0.0219	± 0.0892	± 0.0889
	96	Imp.	-7.83%	-13.98%	-12.69%	-12.88%	-15.03%	-21.83%	-13.76%	-12.20%	-11.38%	1.49%	-11.38%										
		± 0.0441	± 0.0429	± 0.0460	± 0.0457	± 0.1097	± 0.1051	± 0.0652	± 0.0598	± 0.0507	± 0.0492	± 0.0463	± 0.0449	± 0.0890	± 0.0829	± 0.0519	± 0.0507	± 0.1227	± 0.1299	± 0.0638	± 0.0632	± 0.0577	± 0.0570
	168	0.0691	0.0650	0.0733	0.0651	0.1235	0.1239	0.0728	0.0706	0.0889	0.0821	0.0762	0.0683	0.1000	0.0931	0.0750	0.0684	0.1766	0.1599	0.0759	0.0745	0.0799	0.0787
ECL	48	0.0030	0.0009	0.0050	0.0042	0.0108	0.0120	0.0085	0.0037	0.0095	0.0025	0.0068	0.0047	0.0046	0.0131	0.0091	0.0053	0.0124	0.0072	0.0053	0.0024	0.0052	0.0050
		± 0.1205	± 0.1225	± 0.1193	± 0.0980	± 0.1851	± 0.1642	± 0.1006	± 0.0978	± 0.1372	± 0.1281	± 0.1571	± 0.1559	± 0.1722	± 0.1262	± 0.1475	± 0.1168	± 0.1765	± 0.1726	± 0.1282	± 0.1169	± 0.1281	± 0.1403
	96	0.0174	0.0162	0.0282	0.01																		